

AD-A105 219

FLORIDA UNIV GAINESVILLE DEPT OF ELECTRICAL ENGINEERING
STUDY OF 1/F NOISE IN SOLIDS. (U)
MAY 81 K M VAN VLIET; E R CHENETTE

F/6 20/12

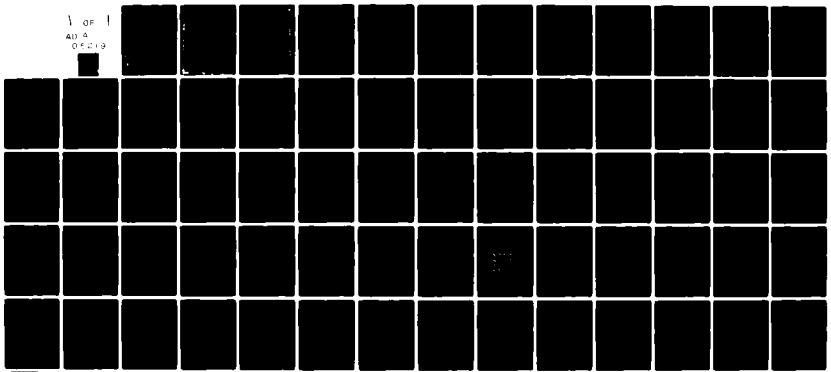
UNCLASSIFIED

AFOSR-80-0050

AFOSR-TR-81-0685

NL

1 of 1
AD-A
04219



END
DATE
FILMED
10-81
DTIC

AD A105219

ONE FILE COPY

78

101

7

6 STUDY OF 1/f NOISE IN SOLIDS.

9 Progress Report, 1 Nov 79-31 May 81

to the

Air Force Office of Scientific Research
Bolling Air Force Base, Washington, D.C. 20332

15 Grant AFOSR-80-0050

16 23 15

Period Covered: November 1, 1979 - May 31, 1981

17 24

Submitted by

19 Karel M. van Vliet Professor
Eugene R. Chenette Professor

DIC
OCT 5 1981

Department of Electrical Engineering
University of Florida
Gainesville, Florida, 32611

11 May 1981 12 65

81 10 2 132

Approved for public release
distribution unlimited.

404825

UNCLASSIFIED

SECURITY CLASSIFICATION OF THIS PAGE (When Data Entered)

REPORT DOCUMENTATION PAGE		READ INSTRUCTIONS BEFORE COMPLETING FORM
1. REPORT NUMBER AFOSR-TR- 81 -0685	2. GOVT ACCESSION NO. AD-A105219	3. RECIPIENT'S CATALOG NUMBER
4. TITLE (and Subtitle) "STUDY OF 1/f NOISE IN SOLIDS"		5. TYPE OF REPORT & PERIOD COVERED <i>Progress Report</i> 1 NOV 79-31 MAY 81 <i>Interim</i>
		6. PERFORMING ORG. REPORT NUMBER
7. AUTHOR(s) Karel M. van Vliet Eugene R Chenette		8. CONTRACT OR GRANT NUMBER(s) AFOSR-80-0050
9. PERFORMING ORGANIZATION NAME AND ADDRESS University of Florida Department of Electrical Engineering Gainesville, FL 32611		10. PROGRAM ELEMENT, PROJECT, TASK AREA & WORK UNIT NUMBERS 2305/C1 61102F
11. CONTROLLING OFFICE NAME AND ADDRESS Air Force Office of Scientific Research/NE Bolling AFB, DC 20332		12. REPORT DATE May 1981
		13. NUMBER OF PAGES 35 + 30 Figures
14. MONITORING AGENCY NAME & ADDRESS (if different from Controlling Office)		15. SECURITY CLASS. (of this report) UNCLASSIFIED
		15a. DECLASSIFICATION/DOWNGRADING SCHEDULE
16. DISTRIBUTION STATEMENT (of this Report) Approved for public release; distribution unlimited		
17. DISTRIBUTION STATEMENT (of the abstract entered in Block 20, if different from Report)		
18. SUPPLEMENTARY NOTES		
19. KEY WORDS (Continue on reverse side if necessary and identify by block number)		
20. ABSTRACT (Continue on reverse side if necessary and identify by block number) This progress report deals with various aspects of the experimental work and the theoretical work performed under this contract. In the introduction we summarize the objectives of the contract. In the experimental work we first describe the two noise-measuring systems which were employed. A Hewlett-Packard digital fast Fourier transform spectral analyser was purchased and adapted for our purpose by writing several computer programs for the output display. Test jigs for devices under test and preamplifiers were build. Further, a real time dual channel correlation spectral analyser was designed and partially built.		

DD FORM 1473
1 JAN 73

EDITION OF 1 NOV 65 IS OBSOLETE

Unclassified
SECURITY CLASSIFICATION OF THIS PAGE (When Data Entered)

UNCLASSIFIED

SECURITY CLASSIFICATION OF THIS PAGE(When Data Entered)

Measurements involving temperature fluctuations and correlations in metal films and in integrated circuit transistors are described. The latter have been recently completed. It is conclusively shown that temperature fluctuations are not the cause of $1/f$ noise in these devices. Under the heading of theoretical work an extensive analysis is presented of noise in diffusion systems. Several analytical models, not considered before, have been solved and the noise is presented. It is conclusively shown that volume (bulk) diffusion noise, whether based on the physical diffusion source or on Voss and Clarke's P-source, never leads to $1/f$ -type spectra. However, surface fluctuations as, e.g., caused by stochastic surface generation-recombination processes, can give rise to many decades of $1/f$ noise. This is worked out in detail for a MOSFET structure. We conclude, therefore, that the large noise observed in MOSFETs can be due to carrier number fluctuations subject to diffusion; at low frequencies the MacWhorter-van der Ziel model may be operative, whereas at higher frequencies our model takes over. Finally, in the theory section we present a novel derivation of quantum $1/f$ noise, occurring in emission processes.

Accession For	
NTIS GRA&I	<input checked="" type="checkbox"/>
DTIC TAB	<input type="checkbox"/>
Unannounced	<input type="checkbox"/>
Justification	
Distribution/	
Availability Codes	
A	

Unclassified
SECURITY CLASSIFICATION OF THIS PAGE(When Data Entered)

Abstract

This progress report deals with various aspects of the experimental work and the theoretical work performed under this contract.

In the introduction we summarize the objectives of the contract.

In the experimental work we first describe the two noise-measuring systems which were employed. A Hewlett-Packard digital fast Fourier transform spectral analyser was purchased and adapted for our purpose by writing several computer programs for the output display. Test jigs for devices under test and preamplifiers were built. Further, a real time dual channel correlation spectral analyser was designed and partially built.

Measurements involving temperature fluctuations and correlations in metal films and in integrated circuit transistors are described. The latter have been recently completed. It is conclusively shown that temperature fluctuations are not the cause of $1/f$ noise in these devices.

Under the heading of theoretical work an extensive analysis is presented of noise in diffusion systems. Several analytical models, not considered before, have been solved and the noise is presented. It is conclusively shown that volume (bulk) diffusion noise, whether based on the physical diffusion source or on Voss and Clarke's P-source, never leads to $1/f$ -type spectra. However, surface fluctuations as, e.g., caused by stochastic surface generation-recombination processes, can give rise to many decades of $1/f$ noise. This is worked out in detail for a MOSFET structure. We conclude, therefore, that the large noise observed in MOSFETs can be due to carrier number fluctuations subject to diffusion; at low frequencies the MacWhorter-van der Ziel model may be operative, whereas at higher frequencies our model takes over.

Finally, in the theory section we present a novel derivation of quantum $1/f$ noise, occurring in emission processes.

List of Figures

1. Transistor test circuit for low-frequency digital spectral analyser.
2. One-third octave display of base channel noise for transistor 2N3945 #1.
3. One-third octave display of collector channel noise for transistor 2N3945 #1.
4. Block diagram for real time correlation measurement system.
5. Two-stage FET low-noise amplifier.
- 5A. Active load low-noise preamplifier.
6. First main amplifier.
- 6A. Second main amplifier.
7. Layout of films for correlation measurements.
8. Noise spectrum of aluminum film at 1.171 mA.
9. Noise spectrum of aluminum film at 1.071 mA.
10. Noise spectrum of aluminum film at 260 μ A.
11. Top view of integrated circuit CA 3018.
- 12 (a). Circuit for thermal transfer function.
(b). Circuit to obtain noise spectra and coherence.
13. Thermal transfer function.
14. Correlation of RCA 3018 NPN transistors.
15. Three-transistor heat-transfer measurement setup.
16. Thermal transfer function for the two "sensors."
17. Correlation (coherence factor) of the two "sensors."
18. Noise of the two "sensor" transistors.
19. Correlation (coherence factor) of the two "sensor" transistors.
20. Low-frequency one-third octave display of base channel noise for 2N3945 #1 (see also Fig. 2).
21. Low-frequency one-third octave display of collector channel noise for 2N3945 #1 (see also Fig. 3).
22. Low-frequency coherence between collector channel and base channel noise for 2N3945 #1.

23. Intermediate frequency coherence between collector channel and base channel noise for 2N3945 #1.
24. Noise for embedded sphere; no volume sources $\eta \neq 0$.
25. Noise for nonembedded sphere $\eta = 0$.
26. Noise for nonembedded sphere $\eta \neq 0$.
27. Noise spectra for nonsymmetrical bar based on Voss and Clarke's P-source.
28. Noise spectra for nonsymmetrical bar based on the physical diffusion source.
29. Noise spectra for disc and square bar based on the physical diffusion source.
30. Noise spectra for a MOSFET due to stochastic surface generation-recombination processes.

TABLE OF CONTENTS

	<u>Page</u>
Abstract	2
List of Figures	3
A. Introduction	6
B. Experimental Work	
I. Construction of Spectral Analyzers (R.R. Schmidt)	8
II. Temperature Fluctuations and Correlation in Thin Films and Integrated Circuit Transistors (J. Kilmer and J.J. Lin)	11
III. Base-Collector Noise Correlations in Transistors (R.R. Schmidt)	15
C. Theoretical Work	
I. Transport Noise (K.M. van Vliet & H. Mehta) . .	16
II. On the Theory of Quantum $1/f$ Noise (P.H. Handel, K.M. van Vliet, and A. van der Ziel)	28
D. Publications and Theses Resulting from the Contract	33
E. References	34

A. Introduction

Whereas many noise phenomena, like shot noise, thermal noise and generation recombination noise, are well understood, $1/f$ noise remains an enigma. This noise has been observed in all semiconductors, metal films, and semiconductor devices. Besides, this noise has been found in electrolyses and membranes, in biomedical phenomena, etc. Though some investigators believe that there must be some universal phenomenon operative in all these manifestations, like scale invariance (S. Macklup [1]), we believe that the ultimate explanation will require the involvement of specific noise causes, as for any other type of noise. This does not mean that general principles, like scale invariance, or nonlinear coupling (Handel et al. [2]) are irrelevant. However, there must be physical mechanisms underlying these mathematical descriptions.

To date there are four serious contenders in the theoretical arena. First, there are still many attempts to explain $1/f$ noise in terms of diffusion-like transport phenomena. In particular, the possibility of temperature fluctuations as the cause of noise in metal films has been often suggested in the recent past, notably by Voss and Clarke in 1976 [3] and later by the Chicago group of Hover et al. [4-6]. The possibility of obtaining $1/f$ noise from surface initiated heat transfer was examined prior to this grant by van Vliet, van der Ziel and Schmidt [7]. A very complete further investigation of the possible connection of diffusion noise and $1/f$ noise was made under this grant by Mehta and van Vliet [8]; see Part C of this report.

Second, there are still attempts to explain $1/f$ noise in terms of number fluctuations, e.g., due to tunneling to deep traps and "slow surface states," as in the van der Ziel-McWhorter theory [9]. In this case the scale invariance of $1/f$ noise stems from the very large distribution in lifetimes with probability $P(\tau) - \text{constant} / \tau$. This type of theory might

be applicable to $1/f$ noise in MOSFETs, together with the "fast surface states" mechanism suggested by Mehta and van Vliet [10].

Third, there are many indications to date that in many devices (perhaps MOSFETs excepted) the $1/f$ noise is due to mobility fluctuations. This was first suggested by the pioneering work of Hooge and Gaal [11], Hooge and van Damme [12], and Kleinpenning [13]. So far only one reasonably satisfactory theory has been presented to explain mobility fluctuations in terms of phonon number fluctuations, see Jindal and van der Ziel [14].

Fourth, there is a fundamental $1/f$ noise theory, which attributes the noise to quantum (infrared divergence) effects in scattering, involving either bremsstrahlung or the excitation of other elementary excitations and configurational states or correlated states (Handel, Ngai [15, 16]). This theory also interprets the noise as mobility fluctuations. Many details are, however, poorly understood; in particular, the magnitude of the noise is not easily evaluated quantitatively.

Under the present grant, we have started with the examination of the first hypothesis which involves temperature noise. In part B.II. we describe experiments which investigate the possibility of temperature fluctuations as being the cause of $1/f$ noise in semiconductor devices and films. Though a full investigation in the entire temperature range from 4K to 300K is still underway, the experiments to date indicate clearly that at room temperature the temperature noise hypothesis fails. Similar conclusions have at the same time been reached by two other research groups at Cornell (W. Webb et al. [17] and at the University of Illinois (Weissmann [18])). The concurrently made theoretical studies are reported in Part C.II.

The quest for mobility fluctuations will be aided by the study of $1/f$ noise in near-ballistic submicron devices, obtained from Dr. L. Eastman at Cornell. Under the present grant the amplifiers and correlation noise

equipment for this purpose were constructed, see Part B.I.

The quest for the validity of Handel's quantum $1/f$ noise theory has begun, and the theory is being studied presently under the extension of the OSR grant; the experiments which will be decisive for the rise or fall of this type of theory are described in the extension proposal submitted recently to OSR.

We note that though the grant started in November, 1979, actual measurements were not commenced until spring, 1980, due to the fact that the noise lab was shut down after the leaving of Dr. Rucker when Professor Chenette was at the NSF in Washington. As a consequence, the start was slow, as reflected also by the low rate of dispensing funds. Consequently, a no-cost extension was granted for seven months, bringing the contract period to a close on May 31, 1981.

B. Experimental Work

I. Construction of Spectral Analyzers (R.R. Schmidt)

For transistor noise measurements at low frequencies, two systems were designed. The first was a digital system using a Hewlett-Packard 3582A Spectrum Analyzer which calculates the fast Fourier transform of the time record for frequencies from 20 mHz to 25 kHz. The second system was designed to cover the frequency range, 3 Hz to 30 kHz, using the real-time correlation method.

a. Digital low-frequency system

A transistor bias and preamplifier test circuit is shown in Figure 1. The base of the DUT is AC open-circuited and the collector is AC short-circuited by the use of operational amplifiers in noninverting and inverting configurations, respectively. The preamplifiers are Burr-Brown OPA101CM operational amplifiers which have an equivalent noise resistance of 2K ohms

above the $1/f$ noise region. The DUT operating point can be controlled by the variable potentiometer which determines the base voltage. To achieve maximum low-frequency response, coupling capacitors have been avoided.

The noise spectra of a 2N3945 npn BJT are shown in Figures 2 and 3. The high frequency plots include a flat region and excess noise regions. These measurements are further described in detail in Section B.III. of this report. Suffice it here to say that later on better representations for displaying the $1/f$ noise were developed.

b. Real-time correlation system

A block diagram of the real-time correlation method measurement system is shown in Figure 4. There are two parallel amplification channels, the outputs of which are multiplied using a four-quadrant multiplier. The result is averaged and read out on a DC voltmeter. This system operates at a single frequency determined by the bandpass filter. It is desired to build a parallel array of these systems operating at various frequencies from a few Hertz to 30 kiloHertz. At present a prototype adjustable single-frequency system has been constructed using Spencer-Kennedy Laboratories, Inc. model 302 dual-channel variable electronic filters. Since these filters accept high-level input signals, in the prototype system they have been moved after the second main amplifier and before the multiplier in each channel. This also reduces the effect of 60 Hz hum at the output of the filters.

The two-stage FET preamp is shown in Figure 5. The FETs are n-channel 2N4393s with high g_m and low noise. The switch S_1 allows the noise figure of the preamp to be accurately measured by comparing the noise at the output due to thermal noise at the input of various resistors. In addition, there is a direct input for very low-level signals of magnitude the order

of 100 nanovolts. The power supply V_{DD} must be capable of delivering 20 milliamperes at about 250 volts with very good regulation. Hum and noise introduced at this state is greatly amplified. The 40-kohm load resistors dissipate two watts each. The low-frequency response of the system is limited by coupling capacitors in this and other stages.

An alternate low-noise preamplifier is shown in Figure 5A. The input stage is a 2N5087 pnp transistor in the common emitter configuration with an active load. The resulting gain is about 70 db. A JFET source follower using an n channel 2N4393 with very high input impedance directly couples the amplified signal to an output stage consisting of an emitter follower which uses a high β npn 2N5088. Only the JFET stage is resistively loaded. This preamp has much lower power consumption than the previous preamp.

The first main amplifier is shown in Figure 6. It uses a Burr Brown model OPA102CM low-noise FET input stage operational amplifier in non-inverting configuration. This results in a high-input impedance that does not load the preamplifier output and thus yields higher gain. The gain is set to about 60 decibels. The bandpass filter in the final system will be a low-level active filter using operational amplifiers or discrete devices. The variable attenuators in the prototype system are Hewlett-Packard model 350Ds which will be replaced by smaller built-in units in the final system.

The second main amplifier is similar to the first except for a few differences as shown in Figure 6A. There is a 600-ohm resistor at the input to match the output impedance of the attenuator. A 741-type operational amplifier may be used since the signal levels in this case are much greater than the background noise.

The multiplier and detector used in this system may be the same as is used in the high-frequency correlation system.

Under the extended contract these dual-channel analyzers are being completed.

II. Temperature Fluctuations and Correlation in Thin Films and Integrated Circuit Transistors (J. Kilmer & J.J. Lin)

a. Noise in aluminum films

Aluminum films of the configuration of Fig. 7 were prepared. The thickness of the film was approximately $20 \overset{\circ}{\text{A}}$. With the other dimensions as in Fig. 7, and a specific resistivity of $2.5 \times 10^{-6} \Omega \text{ cm}$, one finds that the resistance is of the order of $4 \text{ k}\Omega$, as was observed. Some typical noise spectra of one of the films are given in Figs. 8-10. For Fig. 8 (I - $1171 \mu\text{A}$) we find at 16 hz with $\Delta f \approx 11 \text{ hz}$:

$$S_V = \frac{(10^{-100.3/20})^2}{11} = 8.4 \times 10^{-12} \text{ V}^2/\text{hz}$$

With a mobility of $300 \text{ cm}^2/\text{V}_{\text{sec}}$, we find that the density n_0 and the number of carriers in the sample N_0 are: $n_0 \approx 8 \times 10^{21} \text{ cm}^{-3}$, $N_0 \approx 7.5 \times 10^{10}$.

Thus Hooge's constant follows from

$$S_V = \frac{\alpha V^2}{f N}, \quad \text{or} \quad \alpha = \frac{S_V f N}{V^2}$$

We find $\alpha \approx 0.46$. This is two orders of magnitude higher than the commonly accepted value of α . We therefore attribute the noise to the silver paste contacts to these very thin films. Alternately, the noise may be due to an oxide layer which often is present on aluminum films.

The correlation between the two films proved to be negligible over the entire frequency range. This is what would be expected if the noise is due to the contacts or due to an oxide layer (McWhorter model).

Similar noise measurements have been made on tantalum nitride films. The spectra were $1/f$. No correlation measurements on these films have been made as yet due to technical problems in producing closely spaced films.

b. Noise in thermally coupled integrated circuit transistors; two transistor experiments

Voss and Clarke [3] conducted correlation experiments between two adjacent parts of a metal film. From the observed large correlation they concluded that the noise was in agreement with the temperature noise hypothesis. However, if the noise is really due to temperature fluctuations, one should be able to observe a large positive correlation between thermally coupled but electrically isolated parts of a test object.

To test the temperature hypothesis, we examined the noise and thermal response of closely spaced transistors of several RCA CA3018 general purpose integrated circuit chips. One chip contains, among others, two separate transistors and a Darlington pair. The centers of the separate transistor circuits are about $200 \mu\text{m}$ removed from the Darlington circuit; the mutual distance of the separate transistors is about $20 \mu\text{m}$, see Fig. 11. First we examined the mutual thermal response of the two separate transistors by using one transistor as a "heater" and the other one as a "sensor," see Fig. 12.(a). A sinusoidally varying signal was fed into the base of one transistor and V_{BE} of the other transistor was monitored; according to the manufacturer, V_{BE} is a sensitive function of temperature. When a heater signal of frequency f_0 was fed into one transistor, the other transistor showed an a.c. voltage v_{BE} of frequency f_0 and $2f_0$. The second harmonic is a consequence of the quadratic heater power $P_0 \langle \cos^2 2\pi f_0 t \rangle$, fed into the heater. A typical thermal transfer function is given in Fig. 13. The turnover is not sharp since the thermal response time

$$\tau_{th} = L^2/\alpha, \quad (1)$$

where $\alpha = \sigma_{th} / \rho c$ is the thermal diffusion constant (σ_{th} is the thermal conductivity, ρ the density, and c the specific heat), is distributed due to the variation in L for different portions of the device. Assuming the most characteristic to be $20 \mu\text{m}$, taking $\rho = 2.3$, $c = 0.7 \text{ Joule / g}^\circ\text{c}$, and $\sigma_{th} = 8 \times 10^{-3} \text{ watt / cm}^\circ\text{c}$, we find $\alpha = 4.8 \times 10^{-3} \text{ cm}^2/\text{sec}$, $\tau_{th} = 0.83 \times 10^{-3} \text{ sec}$. This gives a corner frequency of

$$f_0 = 1/2\pi\tau_{th} = 192 \text{ hz} , \quad (2)$$

which is of the right order of magnitude. The shape of the curve of Fig. 13 can, in principle, be found by solving the diffusion equation; the details of such a calculation will appear in the M.Sc. thesis of J. Kilmer.

Next the noise spectrum was measured for the "sensor" transistor, in quiescent condition (no heater voltage to other transistors), using the setup of Fig. 12.(b). The spectrum showed the following ranges:

- 1/f for $f < 60 \text{ hz}$
- $1/f^{1/2}$ for $60 < f < 1000 \text{ hz}$
- 1/f for $1000 < f < 10,000 \text{ hz}$
- white for $f > 10,000 \text{ hz}$

The spectrum of the other transistor (the "heater," but without heater power) was nearly the same. Why the spectra are not 1/f over the full frequency range from 1 hz to 10,000 hz is not understood. The $1/f^{1/2}$ range indicates the possible presence of diffusion noise.

However, the noise is not likely due to temperature diffusion. An order of magnitude calculation of the expected noise if the noise was caused by thermal coupling to temperature fluctuations of the chip, using the calibrated data of the thermal transfer function in Fig. 13, indicates

a much too low noise compared to the observed noise. The details of this calculation will also appear in the M.Sc. thesis of J. Kilmer. That the noise is not due to temperature fluctuations was further substantiated by measuring the cross correlation between the noise of the two transistors, see Fig. 14. The coherence factor ρ is defined as

$$\rho = \langle v_1 v_2 \rangle / \sqrt{\langle v_1^2 \rangle \langle v_2^2 \rangle} \quad (3)$$

As is noted, $\rho < 0.1$ for most frequencies.

c. Noise in thermally coupled integrated circuit transistors; three transistor experiments

The two transistor experiments have the drawback that a strict conclusion about the absence of temperature fluctuations as cause for the observed noise is not possible unless a quantitative estimate is made regarding the expected contribution to the noise and to the correct time coefficient, based on the calibrated thermal transfer function. To circumvent this problem, we devised a three-transistor experiment. In this experiment the Darlington pair was used as a "heater"; the collector voltages of the two other transistors, acting as "sensors," were monitored, see Fig. 15. The transfer function for each sensor with respect to the Darlington pair heater is given in Fig. 16. The turnover frequency of the response is now of the order of 2hz, in agreement with the fact that the transfer distance $L \approx 200 \mu\text{m}$ for this experiment.

Next we measured the correlation between the responses of the two sensors. The result is given in Fig. 17. We notice that the coherence factor ρ equals strictly 1 for frequencies below 2hz; above this frequency the phases of the two responses differ due to different thermal delays.

Finally we measured the noise and its correlation for the two sensors under quiescent conditions (no signal to the Darlington heater). The spectra are of the $1/f$ form below 100 hz, see Fig. 18. (At the time of writing

the noise measurements have been extended down to frequencies of 50 mhz, the spectra still being $1/f$.) Lastly, the coherence factor for the noise of the two separate transistors, used as sensors before, is given in Fig. 19. Clearly, $\rho < 0.02$.

The coherence of the noise as given in Fig. 19 can now be directly compared with the coherence obtained by externally induced temperature fluctuations as found in Fig. 14. Clearly, the coherence must be the same for all temperature fluctuations, whether externally induced or spontaneously occurring, since the small signal parameters for the response are the same. Since $\rho(\text{Fig. 19}) \ll \rho(\text{Fig. 14})$, we conclude that the noise cannot be due to spontaneous temperature fluctuations of the integrated circuit or of its thermally connected parts. Thus temperature noise can be excluded as a cause for the $1/f$ noise.

The three-device experiment is clearly a very powerful tool to investigate temperature fluctuations. The experiments are presently being repeated for three thermally coupled gold films of submicron dimensions, manufactured for us by Dr. E. Wolf of the Cornell Submicron facility. These experiments will then be done for all temperatures from 4 K - 300 K. This should settle the uncertainties about the effect of temperature fluctuations as possible cause for $1/f$ noise.

III. Base-Collector Noise Correlations in Transistors (R.R. Schmidt)

To further test the usefulness of the possibility for measuring the coherence factor of two noise inputs with the Hewlett-Packard digital analyzer, we measured the base noise, collector noise, and their coherence for a 2N3945 common emitter bipolar transistor. The results of the single-channel noise spectra are shown in Figs. 20 and 21. We note that there are two low-frequency noise regions. Above 1 hz the excess noise goes as $f^{-2/3}$,

both for the base and collector noise. Below 1 hz the base noise rises faster, viz., as $f^{-3/2}$, whereas the collector noise levels off.

The coherence factor for these two noise spectra is given in Figs. 22 and 23. We note that the coherence below 1 hz is rapidly going to zero, whereas above 1 hz the correlation is nearly unity, diminishing again at high frequencies since white noise then comes into play.

The coherence factor indicates that entirely different noise mechanisms operate below 1 hz and above 1 hz. Thus the measurement of the coherence factor is a powerful tool to separate noise phenomena, to find the limits of the range of a given noise phenomenon. This is particularly important for the ubiquitous $1/f$ noise, of which it is usually assumed that no lower or upper bound occurs. In the transistors shown the correlated $1/f$ -type noise occurs only above frequencies of 1 hz, up to the white noise regime (several kilohertz).

C. Theoretical Work

I. Transport Noise (K.M. van Vliet and H. Mehta)

a. Survey of transport noise

A survey of transport noise methods, involving Green's function procedures and eigenfunction expansions, is appearing in Physica Status Solidi (b) [19].

b. Noise of symmetrical embedded bodies

The noise of symmetrical embedded bodies can be found in closed form using the Green's function procedure. According to a formula of van Vliet and Fassett [20], the noise spectrum of a quantity X, subject to transport in a domain D_s of volume V_s , is given by

$$S_X(\omega) = \frac{4 \text{ var } X}{V_s} \text{Re} \int_{D_s} \int_{D_s} G(r, i\omega, r') d^3r d^3r' \quad (4)$$

where G is the Fourier-Laplace transformed Green's function of the transport equation, typically the diffusion equation. For a circular or cylindrical domain the solution was obtained by MacFarlane [21], Burgess [22], and by van Vliet and Chenette [23]. For a sphere involving diffusion as well as volume generation-recombination, the spectra were hitherto unknown. The problem was solved by Mehta and van Vliet under the present contract.

Thus, we consider a sphere embedded in an infinite domain. The diffusion equation reads

$$\frac{dx}{dt} + \alpha x - D\nabla^2 x = 0, \quad (5)$$

where $\alpha = \tau^{-1}$ is the reciprocal volume lifetime. The Green's function satisfies the Fourier-Laplace transformed equation

$$-\frac{s}{D} G(r,s,r') - \frac{\alpha}{D} G(r,s,r') + \nabla^2 G(r,s,r') = -\frac{1}{D} \delta(r-r') \quad (6)$$

or

$$(\kappa^2 + \nabla^2) G(r,s,r') = -\frac{1}{D} \delta(r-r') \quad (7)$$

where

$$\kappa = i \sqrt{\frac{\alpha + s}{D}} \equiv i \sqrt{\frac{\alpha + i\omega}{D}}. \quad (8)$$

For a spherical coordinate system we have

$$\nabla^2 = \frac{1}{r^2} \frac{\partial}{\partial r} \left(r^2 \frac{\partial}{\partial r} \right) + \frac{1}{r^2 \sin^2 \theta} \frac{\partial^2}{\partial \phi^2} + \frac{1}{r^2 \sin \theta} \frac{\partial}{\partial \theta} \left(\sin \theta \frac{\partial}{\partial \theta} \right). \quad (9)$$

With the conditions that G goes as $\frac{1}{R}$ for $R \rightarrow 0$ (where $R = |r-r'|$) and

$$\lim_{\kappa \rightarrow -\infty + i\infty} G_{\kappa}(R) = 0,$$

one obtains

$$G_{\kappa}(R) = e^{i\kappa R} / 4\pi R D \quad (10)$$

To find the spectrum one must now perform the integration as required by (4):

$$I = \int_{V_s} \int_{V_s} d^3r d^3r' G_{\kappa}(R), \quad (11)$$

where

$$R = \sqrt{r^2 + r'^2 - 2rr' \cos(\theta - \theta')} \quad (12)$$

and

$$\begin{aligned} d^3r &= r^2 \sin \theta d\theta d\phi \\ d^3r' &= r'^2 \sin \theta' d\theta' d\phi' \end{aligned} \quad (13)$$

One may choose $\theta' = 0$. After much algebra the integral is found to be

$$I = \frac{4}{\kappa D i} \left[\frac{a^2 e^{2i\kappa a}}{-2\kappa^2} + \frac{ae^{2i\kappa a}}{i\kappa^3} + \frac{e^{2i\kappa a}}{2\kappa^4} + \frac{a^3}{3i\kappa} - \frac{a^2}{2\kappa^2} - \frac{1}{2\kappa^4} \right], \quad (14)$$

where a is the radius of the sphere. For the spectrum of the total number of holes one obtains, with $X \equiv P \equiv \int x d^3r$:

$$S_{\Delta P} = \text{Re} \frac{64\pi p_0 a^5}{D\phi^5} \left[e^{\phi}(\phi^2 - 4\phi + 4) + \left(\frac{\phi^3}{3} + \phi^2 - 4\right) \right], \quad (15)$$

where $\phi = 2i\kappa a$, κ being given by (8).

We first considered $\alpha = 0$ (pure diffusion). The result is then

$$\begin{aligned} S_{\Delta P} = \frac{16\pi a^5 p_0}{D\gamma^5} \left\{ -2 + \gamma^2 + e^{-\gamma} [\gamma^2(\sin \gamma + \cos \gamma) \right. \\ \left. + 4\gamma \cos \gamma + 2(\cos \gamma - \sin \gamma)] \right\}, \quad (16) \end{aligned}$$

where $\gamma = 2a\sqrt{\omega/2D}$. The spectrum is plotted in Fig. 24, see the $\eta = 0$ curve. The results show a plateau and an $\omega^{-3/2}$ asymptote, as expected from the work of Lox and Orengert [24]. For diffusion with sinks the result is

$$S_{\Delta P}(\omega) = \frac{16\pi a^5 p_0 (\beta^2 - \delta^2)}{3D(\beta^2 + \delta^2)^2} + \frac{16\pi a^5 p_0 K}{D(\beta^2 + \delta^2)^5} \quad (17)$$

where

$$\begin{aligned} K = & (10\beta^2\delta^3 - 5\beta^4\delta - \delta^5) [2\beta\delta + 2\delta e^{-\beta} \cos \delta(\beta + 2) \\ & + e^{-\beta} \sin \delta(\delta^2 - \beta^2 - 4 - 4\beta)] - (\beta^5 - 10\beta^3\delta^2 + 5\beta\delta^4) \\ & \times [\beta^2 - \delta^2 + 2\delta e^{-\beta} \sin \delta(\beta + 2) + e^{-\beta} \cos \delta(\beta^2 - \delta^2 + 4 - 4\beta) - 4]. \end{aligned} \quad (18)$$

and

$$\beta = \frac{2a}{\sqrt{D}} \left[\sqrt{\frac{1}{2} \alpha + \frac{1}{2} \sqrt{\alpha^2 + \omega^2}} \right] \quad (19)$$

$$\delta = \frac{2a}{\sqrt{D}} \left[\sqrt{-\frac{1}{2} \alpha + \frac{1}{2} \sqrt{\alpha^2 + \omega^2}} \right]. \quad (20)$$

Furthermore, the following dimensionless quantities were used:

$$u = \omega\tau_d, \quad (\tau_d = a^2/D \text{ is the diffusion time}), \quad (21a)$$

$$\eta = \tau_d/\tau_v = \alpha\tau_d, \quad (21b)$$

$$\beta = \sqrt{2} \sqrt{\eta + \sqrt{\eta^2 + u^2}}, \quad (21c)$$

$$\delta = \sqrt{2} \sqrt{-\eta + \sqrt{\eta^2 + u^2}}. \quad (21d)$$

The spectra appear in Fig. 22, curves for $\eta \neq 0$.

One notices the occurrence of an ω^{-2} range, in addition to the plateau and $\omega^{-3/2}$ range. It is concluded that the spectra do never resemble a $1/f$ spectrum.

c. Nonembedded sphere

Next we considered the noise in a sphere, on the boundary of which we have surface recombination. The boundary condition is then

$$D \frac{\partial}{\partial n} G(r = a, s, r') + \sigma G(r = a, s, r') = 0 \quad (22)$$

where n denotes the outer normal and σ is the surface recombination velocity.

The differential equation for the Green's function is

$$\begin{aligned} \frac{\partial^2 G}{\partial r^2} + \frac{2}{r} \frac{\partial G}{\partial r} + \kappa^2 G + \frac{1}{r^2} \left[\frac{1}{\sin \theta} \frac{\partial}{\partial \theta} \left(\sin \theta \frac{\partial}{\partial \theta} \right) \right. \\ \left. + \frac{1}{\sin^2 \theta} \frac{\partial^2}{\partial \phi^2} \right] G = -\frac{1}{D} \delta(r - r'), \end{aligned} \quad (23)$$

where κ is the same as in Eq. (8). Using an expansion in spherical polynomials, the solution of (23) subject to (22) can be shown to be

$$\begin{aligned} G(r, r') = \frac{\kappa i}{4\pi D} \sum_{\ell, m} \frac{(2\ell + 1)(\ell - |m|)!}{(\ell + |m|)!} P_{\ell}^m(\cos \theta) e^{im(\phi - \phi')} \\ \times \left[j_{\ell}(\kappa r) h_{\ell}^{(1)}(\kappa r') - j_{\ell}(\kappa r) j_{\ell}(\kappa r') Q_{\ell}(\kappa a) \right], \end{aligned} \quad (24)$$

where

$$Q_{\ell}(\kappa a) = \frac{D\kappa h_{\ell+1}^{(1)}(\kappa a) - \left(\sigma + \frac{D\ell}{a}\right) h_{\ell}^{(1)}(\kappa a)}{D\kappa j_{\ell+1}(\kappa a) - \left(\sigma + \frac{D\ell}{a}\right) j_{\ell}(\kappa a)}, \quad (25)$$

and where j_{ℓ} is the spherical Bessel function of order ℓ , $h_{\ell}^{(1)}$ is the spherical Hankel function of the first kind of order ℓ .

We must now perform a six-fold integration, as required by (4). The integral is obtainable in closed form, by employing the addition theorem

$$\frac{j_\ell i\kappa R}{i\kappa R} = \sum_{\ell=0}^{\infty} (2\ell+1) j_\ell(\kappa r) h_\ell^{(1)}(\kappa r) P_\ell(\cos \theta). \quad (26)$$

After a very laborious calculation (see the Ph.D. dissertation of Mehta for details) one obtains

$$S_p(\omega) = \frac{4(\text{var } P)}{D} \text{Re } \Psi(\omega), \quad (27)$$

where

$$\Psi(\omega) = \frac{1}{\eta + iu} \left[1 - \frac{3j_1(i\sqrt{\eta + iu})}{\xi(\eta + iu)j_1(i\sqrt{\eta + iu}) + i\sqrt{\eta + iu}j_0(i\sqrt{\eta + iu})} \right] \quad (28)$$

where η and u are defined as in (21a) and (21b), while

$$\xi = \tau_s / \tau_d, \quad \tau_d = a^2/D, \quad \tau_s = a/\sigma.$$

Here τ_s is the surface recombination time and τ_d is the diffusion time.

When there are no volume sinks, $\eta = 0$. Using the relations for spherical Bessel functions,

$$\begin{aligned} j_0(z) &= \sin z / z, \\ j_1(z) &= \sin z / z^2 - \cos z / z, \end{aligned} \quad (29)$$

we obtained

$$\text{Re } \Psi(\omega) = \frac{3(AD + BC)}{4\alpha^4 \xi(C^2 + D^2)} \quad (30)$$

where $\alpha = \sqrt{u/2}$ and where

$$A = (-\sin \alpha \cosh \alpha + \alpha \cos \alpha \cosh \alpha + \alpha \sin \alpha \sinh \alpha) \quad (31a)$$

$$B = (\cos \alpha \sinh \alpha + \alpha \sin \alpha \sinh \alpha - \alpha \cos \alpha \cosh \alpha) \quad (31b)$$

$$C = (\cos \alpha \sinh \alpha + \alpha \sin \alpha \sinh \alpha - \alpha \cos \alpha \cosh \alpha - \frac{\cos \alpha \sinh \alpha}{\xi}) \quad (31c)$$

$$D = (-\sin \alpha \cosh \alpha + \alpha \cos \alpha \cosh \alpha + \alpha \sin \alpha \sinh \alpha + \frac{\sin \alpha \cosh \alpha}{\xi}) \quad (31d)$$

For various values of the parameter ξ the spectra are plotted in Fig. 25.

In contrast to the embedded sphere, the high frequency slope is always ω^{-2} .

When both volume and surface g-r processes play a role, $\eta \neq 0$, $\xi \neq 0$.

The following result is found after considerable algebra:

$$\text{Re } \Psi(\omega) = \frac{\xi(MP + NQ) - 3(AM + BN)}{\xi \{ (\bar{\beta}^2 P + \bar{\delta}^2 P)^2 + (\bar{\beta}^2 Q + \bar{\delta}^2 Q)^2 \}} \quad (32)$$

where

$$\bar{\beta} = (1/\sqrt{2}) \sqrt{\eta + \sqrt{\eta^2 + u^2}} \quad (33)$$

$$\bar{\delta} = (1/\sqrt{2}) \sqrt{-\eta + \sqrt{\eta^2 + u^2}} \quad (34)$$

$$A = (-\sin \bar{\delta} \cosh \bar{\beta} + \bar{\delta} \cos \bar{\delta} \cosh \bar{\beta} + \bar{\beta} \sin \bar{\delta} \sinh \bar{\beta}) \quad (35a)$$

$$B = (\cos \bar{\delta} \sinh \bar{\beta} - \bar{\beta} \cos \bar{\delta} \cosh \bar{\beta} + \bar{\delta} \sin \bar{\delta} \sinh \bar{\beta}) \quad (35b)$$

$$C = A + \frac{\sin \bar{\delta} \cosh \bar{\beta}}{\xi} \quad (35c)$$

$$D = B - \frac{\cos \bar{\delta} \sinh \bar{\beta}}{\xi} \quad (35d)$$

$$P = (\bar{\beta}^2 - \bar{\delta}^2) C - 2\bar{\beta}\bar{\delta} D \quad (35e)$$

$$Q = (\bar{\beta}^2 - \bar{\delta}^2) D + 2\bar{\beta}\bar{\delta} C \quad (35f)$$

$$M = (\bar{\beta}^2 - \bar{\delta}^2) P - 2\bar{\beta}\bar{\delta} Q \quad (35g)$$

$$N = (\bar{\beta}^2 - \bar{\delta}^2) Q + 2\bar{\beta}\bar{\delta} P \quad (35h)$$

The low-frequency plateau is

$$\lim_{\omega \rightarrow 0} \overline{\text{Re}} \Psi(\omega) = (1 + 5\xi) / 15 \quad (36)$$

The high-frequency asymptote is, noticing $\bar{\beta} \sim \bar{\delta} \sim \sqrt{u/2}$,

$$\text{Re} \Psi(\omega) \sim 3 / \xi u^2 \quad (37)$$

The possible spectra are plotted in Fig. 26.

Though the details of the spectra are very revealing, we note that the spectra never resemble a $1/f$ spectrum.

d. Nonsymmetrical embedded bodies

The noise was also calculated for a nonsymmetrical embedded rectangular bar of dimensions $L_1 \times L_2 \times L_3$. In this case the Green's function cannot be obtained in closed form, and the eigenfunction expansion technique is preferable. Let S be the spectrum of the volume noise source. We then obtain

$$S(\omega) = \frac{1}{(2\pi)^3} \int_{-\infty}^{\infty} \int_{-\infty}^{\infty} d^3k d^3k' \frac{\left| \int_V e^{i\mathbf{k} \cdot \mathbf{r}} d^3r \right|^2}{(Dk^2 + i\omega)(Dk'^2 - i\omega)} \times \int d^3r_1 \int d^3r_2 S_{\xi}(\mathbf{r}_1, \mathbf{r}_2) e^{-i(\mathbf{k} \cdot \mathbf{r}_1 - \mathbf{k}' \cdot \mathbf{r}_2)} \quad (38)$$

For Voss and Clarke's P source,

$$S_{\xi}(\mathbf{r}_1, \mathbf{r}_2) = P_0^2 \delta(\mathbf{r}_1 - \mathbf{r}_2) \quad (39)$$

For the rectangular bar we then obtain

$$S(\omega) = P_0^2 (L_1 L_2 L_3)^2 \int_{-\infty}^{\infty} \frac{d^3k}{D^2 k^4 + \omega^2} \prod_{i=1}^3 \frac{\sin^2(\frac{1}{2} k_i L_i)}{(\frac{1}{2} k_i L_i)^2} \quad (40)$$

For the bar there are break points at $\omega_i = D/L_i^2$. Voss and Clarke claim that the following frequency ranges occur

$$\omega \ll \omega_1: S(\omega) \propto \omega^{-1/2} \quad (40a)$$

$$\omega \ll \omega \ll \omega_2: S(\omega) \propto \omega^{-1} \quad (40b)$$

$$\omega_2 \ll \omega \ll \omega_3: S(\omega) \propto \omega^{-3/2} \quad (40c)$$

$$\omega \gg \omega_3: S(\omega) \propto \omega^{-2} \quad (40d)$$

In order to verify this Eq (40) was rendered in a dimensionless form and put in the computer. The resulting spectrum is given in Fig. 27. We note that only two break points are observable and that no 1/f range occurs.

Voss and Clarke's P source is highly hypothetical. The correct source is the diffusion source:

$$S_{\xi}(\underline{r}, \underline{r}') = 4 D \underline{\nabla} \cdot \underline{\nabla}' n(r) \delta(\underline{r} - \underline{r}') \quad (41)$$

This leads to the result,

$$S(\omega) = \text{constant} \int_{\infty} \frac{d^3k D k^2}{D^2 k^4 + \omega^2} \prod_{i=1}^3 \frac{\sin^2(\frac{1}{2} k_i L_i)}{(\frac{1}{2} k_i L_i)^2}, \quad (42)$$

which differs from (40) by the factor $D k^2$ in the numerator. According to this formula, the following ranges occur:

$$\omega \ll \omega_1: S(\omega) = \text{constant} \quad (43a)$$

$$\omega_1 \ll \omega \ll \omega_2: S(\omega) \propto -\log \omega \quad (43b)$$

$$\omega_2 \ll \omega \ll \omega_3: S(\omega) \propto \omega^{-1/2} \quad (43c)$$

$$\omega \gg \omega_3: S(\omega) \propto \omega^{-3/2} \quad (43d)$$

Again the spectrum was put in a dimensionless form and fed into the computer. The result is given in Fig. 28. The predictions of Eqs (43) are more or less confirmed.

We also evaluated the spectra for a square bar, $L_1 = L_2 \ll L_3$, and a square disc, $L_1 = L_2 \gg L_3$. The results are plotted in Fig. 29.

Again, we conclude from all these computations that the spectra never show a $1/f$ resemblance over many decades.

In conclusion: We established beyond doubt that diffusion noise gives no $1/f$ -like noise spectrum in any geometry, whether embedded or nonembedded for any type of boundary conditions (Dirichlet, Neumann, or mixed). Thus any attempt to explain $1/f$ noise by some diffusion mechanism, with or without volume g-r processes and with or without surface recombination is doomed to failure. See, however, the next subsection for a possible mechanism in MOSFETs.

e. In the above calculations we considered various types of boundary conditions, but the source of the noise was due to diffusion fluctuations and/or volume g-r processes. Next we consider the noise due to surface g-r processes. In this case we have stochastic boundary conditions, i.e., (22) is replaced by,

$$\begin{aligned} D \frac{\partial \Delta p}{\partial x} \Big|_{x=0} - \sigma \Delta p \Big|_{x=0} &= \zeta(t) \\ D \frac{\partial \Delta p}{\partial x} \Big|_{x=w} + \sigma \Delta p \Big|_{x=w} &= \zeta(t) \end{aligned} \tag{44}$$

Note that we consider one-dimensional diffusion in a sample of width w . The volume source ξ will be set $\equiv 0$, since its noise was calculated in the preceding sections (we may consider the noise from the sources ζ - surface - and ξ - volume - separately since these sources are uncorrelated). The one-

dimensional diffusion equation for holes is

$$\frac{\partial \Delta p(x,t)}{\partial \tau} - D \frac{\partial^2 \Delta p(x,t)}{\partial x^2} + \frac{\Delta p(x,t)}{\tau} = 0. \quad (45)$$

Associated with these equations we define the Fourier-Laplace transformed Green's function $G(x,x',i\omega)$ and the surface Green's function $H(x,0,i\omega)$.

For the noise due to the source ζ we obtain

$$S_{\Delta p}(x,x',\omega) = H(x,0,i\omega) H(x',0,-i\omega) S_{\zeta}. \quad (46)$$

The source spectrum is white:

$$S_{\zeta} = 4M\alpha\sigma p_0 / A, \quad (47)$$

where p_0 is the average density of holes, A is the area, σ is the surface recombination velocity, $\alpha = \text{var } p / p_0$ and M is a modulation factor ≥ 1 .

In a MOSFET we must find the averaged fluctuations in the channel of width $W_1 \ll W$. Thus,

$$S_{\Delta p}^-(\omega) = \frac{S_{\zeta}}{\sigma^2} \left| \frac{\sigma}{W_1} \int_0^{W_1} H(x,0,i\omega) dx \right|^2. \quad (48)$$

For the surface Green's function we obtained

$$H(x,0,i\omega) = \frac{1}{\sigma D_r} \left(\sinh \frac{W-x}{L} + \frac{D}{\sigma L} \cosh \frac{W-x}{L} \right), \quad (49)$$

where

$$L = \sqrt{\frac{D}{i\omega + 1/\tau}} \quad (50)$$

and

$$D_r = \left(1 + \frac{D^2}{\sigma^2 L^2} \right) \sinh \frac{W}{L} + \frac{2D}{\sigma L} \cosh \frac{W}{L}. \quad (51)$$

We write $W = W_1 + W_2$ where W_1 is the width of the channel and W_2 is the width of the bulk material of the MOSFET. Carrying out the integration indicated in (48) we find $S_{\Delta p}^-(\omega) \propto |f(i\omega)|^2$, where

$$f(i\omega) = \frac{\frac{L}{W_1} \left[\tanh \frac{W_1}{L} + \frac{D'L}{DL'} \tanh \frac{W_2}{L'} \frac{\cosh \left(\frac{W_1}{L}\right) - 1}{\cosh \left(\frac{W_1}{L}\right)} \right]}{\left[\left(\tanh \frac{W_1}{L} + \frac{D}{\sigma L} \right) \frac{D'L}{DL'} \tanh \frac{W_2}{L'} + 1 + \frac{D}{\sigma L} \tanh \frac{W_1}{L} \right]} \quad (52)$$

Here primed parameters refer to the bulk and unprimed parameters refer to the channel.

At very low frequencies $|W_1/L| \ll 1$ and $|W_2/L'| \ll 1$. Expanding $\tanh(W_1/L) \approx W_1/L$, etc., we find for low frequencies a constant plateau.

At intermediate frequencies $|W_1/L| \ll 1$ but $|W_2/L'| \gg 1$ since $W_2 \gg W_1$. Expanding the appropriate hyperbolic functions, we now find for this range,

$$|f(i\omega)|^2 = \tau_d' / \tau_s'^2 \omega \quad (53)$$

where $\tau_d' = W^2 / D' \approx W_2^2 / D'$ and $\tau_s' = W / \sigma \approx W_2 / \sigma$.

Thus a large 1/f range occurs.

For high frequencies $|W_1/L| \gg 1$ and $|W_2/L'| \gg 1$. One easily confirms that there is an ω^{-2} asymptote. This is confirmed by computer calculations, see Fig. 30. For realistic values of W_1 and W_2 , one finds that the 1/f range, which starts for $\omega \geq 1/\tau$, can continue up to many gigahertz. Thus, this noise which is due to fast surface states continues the noise spectrum due to the slow surface states, occurring for $\omega \leq 1/\tau$. This is the cause that 1/f noise in MOSFETs can occur even for very high frequencies. We note that the results obtained stem from the response of the diffusion equation to surface sources; no distribution of lifetimes needs to be invoked.

Having investigated many diffusion mechanisms, we conclude that 1/f noise seldom occurs, except in the case of a small conducting channel on a large substrate; the 1/f range stems from the diffusion and subsequent recombination in the bulk.

The details of this theory are being published.

II. On the Theory of Quantum 1/f Noise

(P.H. Handel, K.M. van Vliet, and A. van der Ziel)

Under the contract the above-named persons wrote an article on "Superstatistical Emission Noise," now accepted for publication in Physica A. In this article we treated various emission noise problems with compound Poisson statistics, viz.: noise due to emission centers, cathodoluminescence noise, photon noise, and quantum 1/f noise. In essence, quantum 1/f noise is treated here as a wave interaction noise; the wave packet here being of a corpuscular rather than ondular nature, as with photon noise.

Thus, consider a beam of emitted particles (electrons) undergoing scattering in the emission process. Let $m(t)$ be the number of emitted particles per second. The distribution for the emission of M particles in an interval $(t, t + \theta)$ is then written as

$$W(M, \theta) = \sum_{\{m(t)\}} \left[\frac{\int_t^{t+\theta} m(t') dt'}{M} \right]^M e^{-\int_t^{t+\theta} m(t') dt'} P[m(t)] . \quad (54)$$

This compound distribution takes into account that the average number emitted, $\int_t^{t+\theta} m(t') dt'$ is subject to fluctuations due to quantum mechanical uncertainty; $P[m(t)]$ is the probability density functional; $\sum_{\{m(t)\}}$ may also be replaced by the functional integral $\int Dm(t)$ if m is considered to be a continuous variable. We use the bar for averages over M and $\langle \rangle$ for averages involving m . For the variance ΔM_0^2 we find from (54) in a straightforward fashion:

$$\begin{aligned}
 \overline{\Delta M_\theta^2} &= \overline{M_\theta(M_\theta - 1)} - \overline{M_\theta} \overline{(M_\theta - 1)} \\
 &= \overline{M_\theta} + \int_t^{t+\theta} \int_t^{t+\theta} dt_1 dt_2 \langle m(t_1)m(t_2) \rangle - \int_t^{t+\theta} m(t_1) dt_1 \int_t^{t+\theta} m(t_2) dt_2 \\
 &= \theta \langle m \rangle + \int_0^\theta \int_0^\theta \langle \Delta m(t_1) \Delta m(t_2) \rangle dt_1 dt_2 \quad (55)
 \end{aligned}$$

The first term is the shot noise term; the second term will be called "wave-interaction noise" or "intensity-fluctuation noise" (see van Vliet [25]).

By MacDonald's theorem the spectrum $S_m(\omega)$ is related to $\overline{\Delta M_\theta^2}$, according to [noticing that $\theta^{-1} M_\theta = \frac{1}{\theta} \int_t^{t+\theta} m(t') dt' \equiv m_\theta(t)$ is the "short-time average" of $m(t)$]:

$$\begin{aligned}
 S_{\Delta m}(\omega) &= 2\omega \int_0^\infty d\theta \sin \omega\theta \frac{\partial}{\partial \theta} [\theta^2 \overline{\Delta m_\theta^2}] \\
 &= 2\omega \int_0^\infty d\theta \sin \omega\theta \frac{\partial}{\partial \theta} [\overline{\Delta M_\theta^2}] \quad (56)
 \end{aligned}$$

Using (55) this yields two parts. The first part is

$$S_{\Delta m}^I(\omega) = 2\omega \int_0^\infty d\theta \sin \omega\theta \langle m \rangle = 2\langle m \rangle \quad (57)$$

where we used Cauchy's principal value for the improper integral. Thus (57) indicates shot noise.

The second part we write as

$$S_m^{II}(\omega) = 2\omega \langle m \rangle^2 \int_0^\infty d\theta \sin \omega\theta \frac{\partial}{\partial \theta} \int_0^\theta \int_0^\theta \langle \hat{\Delta m}(t_1) \hat{\Delta m}(t_2) \rangle dt_1 dt_2 \quad (58)$$

$\langle \hat{\Delta m}(t_1) \hat{\Delta m}(t_2) \rangle$ is the normalized autocorrelation function of the

intensity-fluctuation noise. With some transformations (see the appendix of the paper for details) one shows that

$$\int_0^\theta \int_0^\theta \hat{\Delta m}(t_1) \hat{\Delta m}(t_2) dt_1 dt_2 = 2 \int_0^\theta du \int_0^u dv \langle \hat{\Delta m}(v) \hat{\Delta m}(0) \rangle . \quad (59)$$

This gives

$$S_m^{II}(\omega) = 4\omega \langle m \rangle^2 \int_0^\infty d\theta \sin \omega\theta \int_0^\theta dv \langle \hat{\Delta m}(v) \hat{\Delta m}(0) \rangle . \quad (60)$$

Integrating once by parts and using the Wiener-Khintchine theorem, we obtain

$$S_{\Delta m}^{II}(\omega) = 4 \langle m \rangle^2 \int_0^\infty d\theta \cos \omega\theta \langle \hat{\Delta m}(\theta) \hat{\Delta m}(0) \rangle = \langle m \rangle^2 \hat{S}_{\Delta m}(\omega) , \quad (61)$$

where $\hat{S}_{\Delta m}(\omega)$ is the normalized intensity-fluctuation noise.

Let now $\Psi(x,t)$ and $\Psi^\dagger(x,t)$ describe the local particle field in the usual way of quantum field theory, being each the sum of a non-scattered beam and a scattered beam. In addition we assume that ψ^\dagger is an analytic signal, obtained by adding to half of the signal one-half of its Hilbert transform. Then the spectrum $S_{\psi^\dagger}(f)$ is zero for negative frequencies. Thus the local density $\psi^\dagger \psi$ can be written as an integral over positive energy losses, $\epsilon = hf$,

$$\langle \psi^\dagger \psi \rangle = \int_0^\infty S_{\psi^\dagger}(\epsilon) d\epsilon ; \quad (62)$$

hence $S_{\psi^\dagger}(\epsilon)$ is both the spectral density of ψ^\dagger and the part of $\langle \psi^\dagger \psi \rangle$ with average energy loss in $(\epsilon, \epsilon + d\epsilon)$, divided by $d\epsilon$. For the latter we have, see Handel [15,16],

$$S_{\psi^\dagger}(\epsilon) = \frac{\delta(\epsilon) + \alpha A (\epsilon/\epsilon_0)^{\alpha A} \epsilon^{-1} u(\epsilon - \epsilon_0)}{1 + \alpha A \int_{\epsilon_0}^{\Lambda} (\epsilon/\epsilon_0)^{\alpha A} \epsilon^{-1} d\epsilon}, \quad (63)$$

where αA is the infrared exponent, u is the unit step function, and $\epsilon_0 = hf_0$ is an energy resolution limit set (arbitrarily) by the lowest measured frequency $f_0 \geq T^{-1}$, T being the duration of the experiment; Λ is the largest possible energy loss, i.e., the kinetic energy $mv^2/2$ of the carriers. The delta term represents the "DC" component of the spectrum, which is therefore affected by the choice of ϵ_0 . Note that (62) is normalized to unity:

$$\langle \psi^\dagger \psi \rangle = \int_0^{\infty} S_{\psi^\dagger}(\epsilon) d\epsilon = \int_{-\infty}^{\infty} S_{\psi^\dagger}(\epsilon) d\epsilon = 1. \quad (62')$$

Now $\hat{m} = \psi^\dagger \psi$, so that $\langle \hat{m} \rangle = 1$ as contended above. For the spectrum of \hat{m} (not an analytic signal) we find by convolution, see van Vliet [25],

$$\begin{aligned} S_{\hat{m}}(f) &= 2 \int_0^{\infty} S_{\psi^\dagger}(\nu) S_{\psi^\dagger}(\nu+f) d\nu \\ &= 2 \int_{-\infty}^{\infty} S_{\psi^\dagger}(\nu) S_{\psi^\dagger}(\nu+f) d\nu \\ &= \frac{2\delta(f) + 4\alpha A (f/f_0)^{\alpha A} f^{-1} u(f-f_0)}{1 + 2\alpha A \int_{f_0}^{\Lambda/h} (f/f_0)^{\alpha A} f^{-1} df} \end{aligned} \quad (64)$$

where a small ("noise of noise") term proportional to $(\alpha A)^2$ has been neglected both in the numerator and in the denominator. Again, the $\delta(f)$ term represents the DC power of the spectrum, for by the Wiener-Khintchine theorem,

$$\begin{aligned}
 S_{\Delta m}^{\wedge}(f) &= 2 \int_{-\infty}^{\infty} e^{-i\omega t} \langle \hat{\Delta m}(t) \hat{\Delta m}(0) \rangle df \\
 &= 2 \int_{-\infty}^{\infty} e^{-i\omega t} \langle \hat{m}(t) \hat{m}(0) \rangle dt - 2 \langle \hat{m} \rangle^2 \int_{-\infty}^{\infty} e^{-i\omega t} dt \\
 &= S_m^{\wedge}(f) - 2 \delta(f) ,
 \end{aligned} \tag{65}$$

where we noted $\langle \hat{m} \rangle^2 = 1$. With $\alpha A \ll 1$, (64) and (65) give

$$S_{\Delta m}^{\wedge}(f) \approx 4 \alpha A (f/f_0)^{\alpha A} f^{-1}, \quad f > f_0 . \tag{66}$$

Substituting into (61) we find for the shot noise plus 1/f noise in the flux $m(t)$:

$$S_{\Delta m}(\omega) = 2 \langle m \rangle + 4 \langle m \rangle^2 \alpha A (f/f_0)^{\alpha A} f^{-1} \approx 2 \langle m \rangle + 4 \langle m \rangle^2 \alpha A / f . \tag{67}$$

This expression ignores, however, the incoherence of the 1/f noise contributions from various carriers in the flux. If n is the concentration of electrons in the cathode of surface area F and λ_0 is the mean free path of the electrons, the number of independent noise contributions is $N = nF\lambda_0$. Hence (67) must be corrected to read

$$S_{\Delta m}(\omega) = 2 \langle m \rangle + 4 \langle m \rangle^2 \alpha A / fN . \tag{68}$$

If $I = em$, then for the current noise,

$$S_{\Delta I}(\omega) = 2 e \langle I \rangle + 4 \langle I \rangle^2 \alpha A / fN . \tag{69}$$

Thus we have a Hooge constant:

$$\alpha_H = 2 \alpha A . \tag{70}$$

For a computation of αA for various infra-quanta, see Handel [16].

D. Publications and Theses Resulting from the Contract

1) M.Sc. Theses

- a) R.R.J. Schmidt: "Various Systems for the Measurement of Noise from 20 Millihertz to 30 Megahertz," University of Florida, March, 1981.
- b) J. Kilmer: In preparation.

2) Ph.D. Dissertation

H. Mehta, "Transport Noise Arising from Diffusion and Bulk or Surface Generation-Recombination," University of Florida, January, 1981.

3) Publications

- a) "Theory of Transport Noise in Semiconductors, A Survey," K.M. van Vliet and H. Mehta, Physica Status Solidi (b), to appear July, 1981.
- b) "Superstatistical Emission Noise," K.M. van Vliet, P.H. Handel and A. van der Ziel, Physica A, in press.
- c) "Absence of Temperature Fluctuations in 1/f Noise Correlation Experiments," J. Kilmer, E.R. Chenette, K.M. van Vliet and P.H. Handel, submitted to Phys. Rev. Letters.
- d) Three papers are in preparation on the work done by H. Mehta and K.M. van Vliet.

E. References

- [1] S. Machlup, "Scale Invariance Implies 1/f Spectrum," Second International Conf. 1/f Noise, Orlando, Florida, 1980, Report (University of Florida), p. 556.
- [2] P.H. Handel et al., "Towards a More General Understanding of 1/f Noise," submitted to Physics Letters .
- [3] R.F. Vos and J. Clarke, Phys. Rev. B13, 556 (1976).
- [4] J.W. Eberhard and P.M. Horn, Phys. Rev. Letters 39, 643 (1977).
- [5] P. Dutta, J.W. Eberhard, and P.H. Horn, Solid State Comm. 27, 1389 (1978).
- [6] P. Dutta, P. Dimon, and P.H. Horn, Phys. Rev. Lett. 43, 646 (1979).
- [7] K.M. van Vliet, A. van der Ziel, and R.R. Schmidt, J. Appl. Phys. 51, 2947 (1980).
- [8] K.M. van Vliet and H. Mehta, "Theory of Transport Noise in Semiconductors, A Survey," Phys. Stat. Solidi (b), in press.
- [9] A. van der Ziel, "Flicker Noise in Electronic Devices," in Advances in Electronics and Electron Physics (L. Martin Ed.), 1979.
- [10] H. Mehta and K.M. van Vliet, to be published.
- [11] F.H. Hooge and J.L.M. Gaal, Philips Res. Rep. 26, 345 (1971).
- [12] F.H. Hooge and L.K.J. van Damme, Phys. Lett. 66A, 315 (1978).
- [13] T.G.M. Kleinpenning, Physica 77, 78 (1974).
- [14] R.P. Jindal and A. van der Ziel, J. Appl. Physics, in press.
- [15] P.H. Handel, Phys. Rev. Lett. 34, 1492, 1495 (1975).
- [16] P.H. Handel, Phys. Rev. 22A, 745 (1980): also Proc. Second Inter. Symposium 1/f Noise, Orlando, Florida, 1980, pp. 42, 56, 96, 525, and 550; K.L. Ngai, *ibid.*, p. 445.
- [17] J.H. Scofield, D.H. Darling and W.W. Webb, Phys. Rev. Letters, submitted.
- [18] M.B. Weissman, Phys. Rev. Letters, submitted.
- [19] See [8] and also Proc. Second Intern. Conf. 1/f Noise, Orlando, Florida, 1980, Report (University of Florida), p. 305.
- [20] K.M. van Vliet and J.R. Fassett, in Fluctuation Phenomena in Solids (R.E. Burgess, Ed.), pp. 267-359.

- [21] G.G. MacFarlane, Proc. Phys. Soc. (London) B63, 807 (1950).
- [22] R.E. Burgess, Proc. Phys. Soc. (London) B66, 334 (1953).
- [23] K.M. van Vliet and E.R. Chenette, Physica 33, 985 (1966).
- [24] M.Lax and P. Mengert, Phys. Chem. Solids 14, 248 (1960).
- [25] K.M. van Vliet, Physica 83 B & C, 52 (1976).

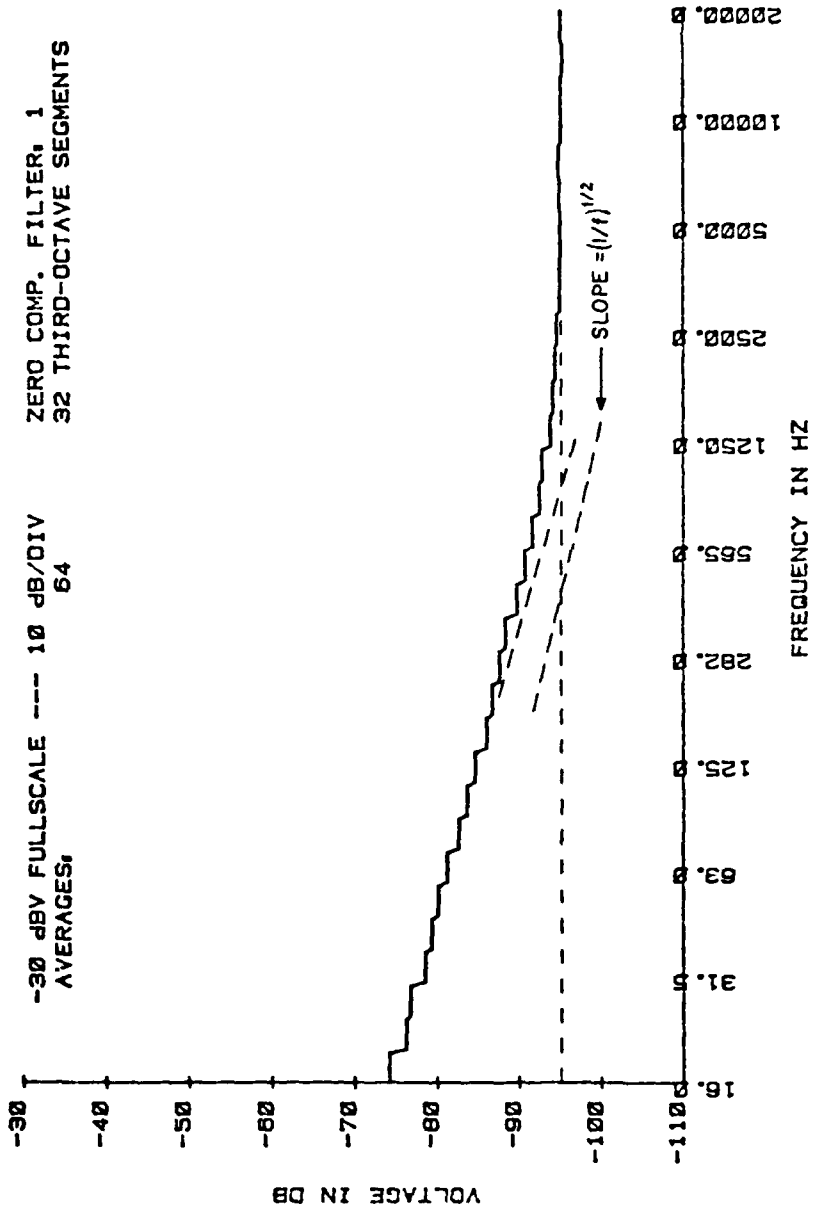


Fig. 3

One-third octave display of collector channel noise for transistor 2N3945 #1.

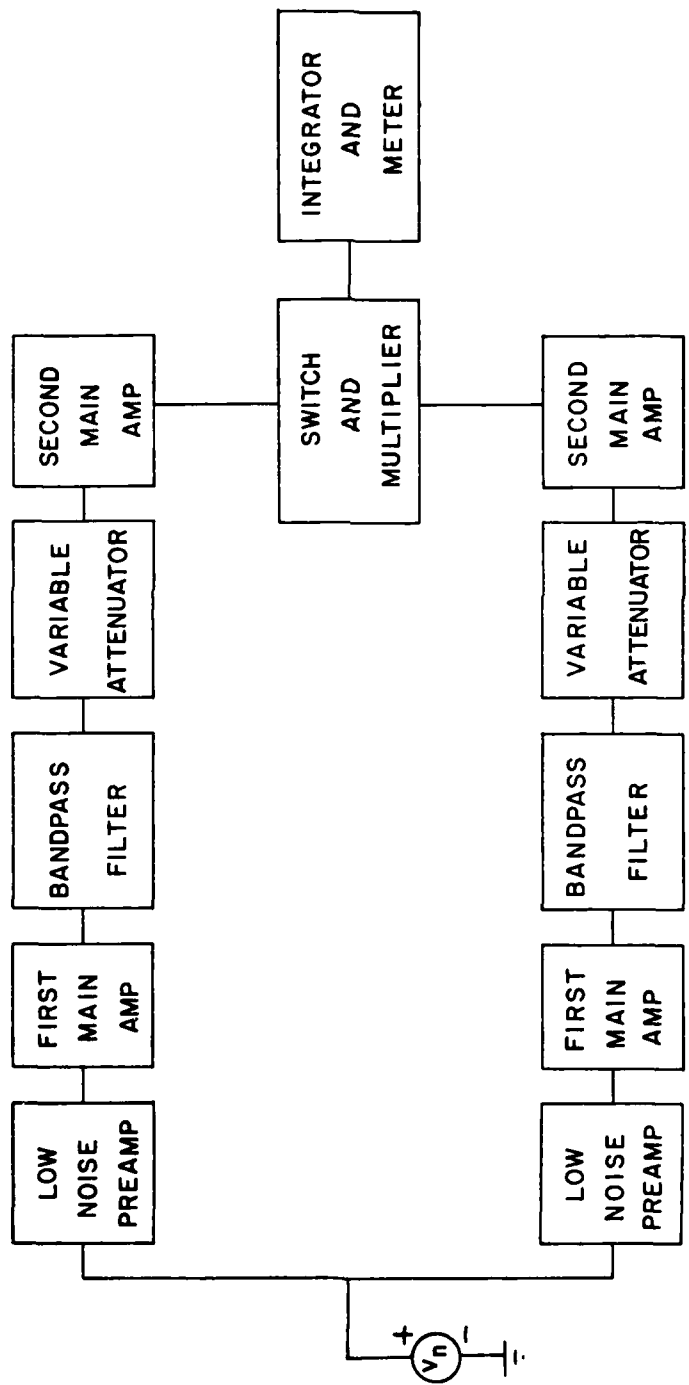


Fig. 4

Block diagram for real time correlation measurement system.

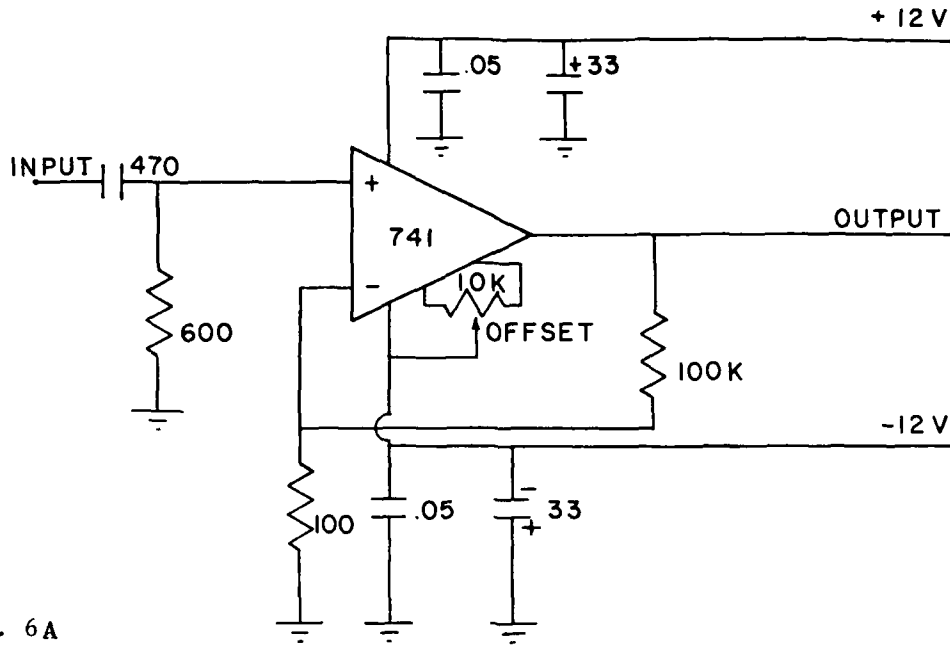


Fig. 6A

Second main amplifier.

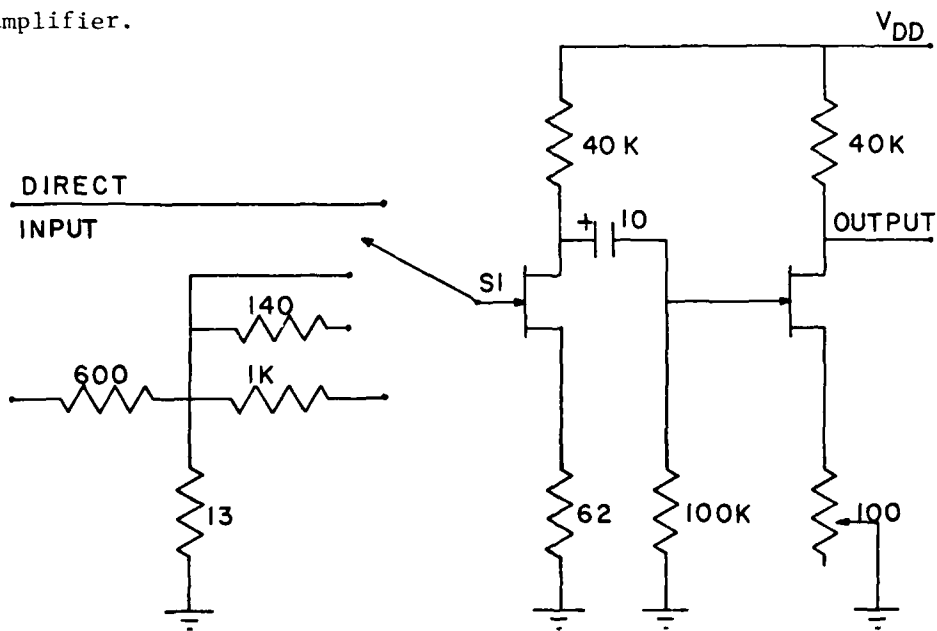


Fig. 5

Two-stage FET low-noise amplifier.

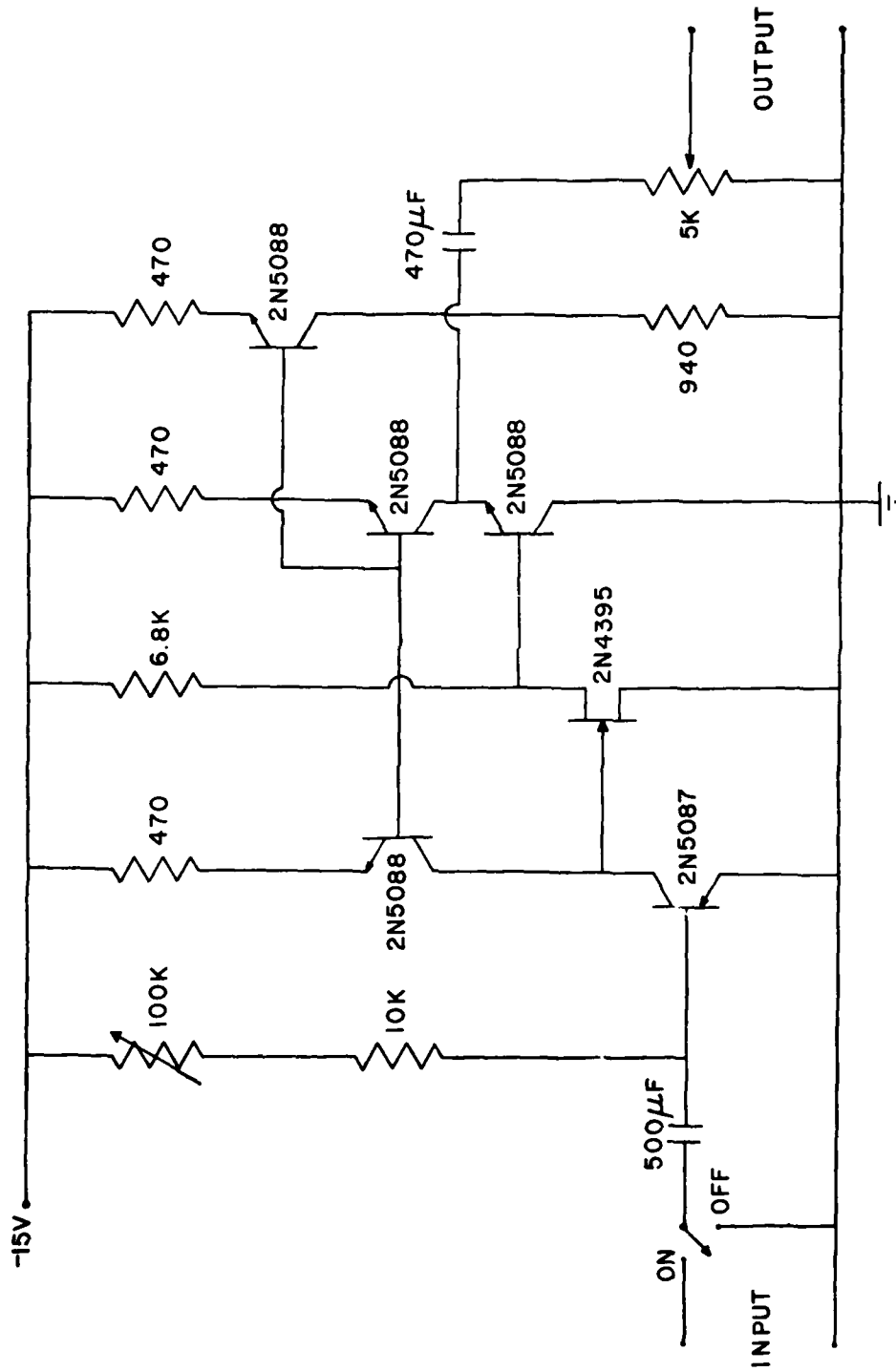


Fig. 5A

Active load low-noise preamplifier.

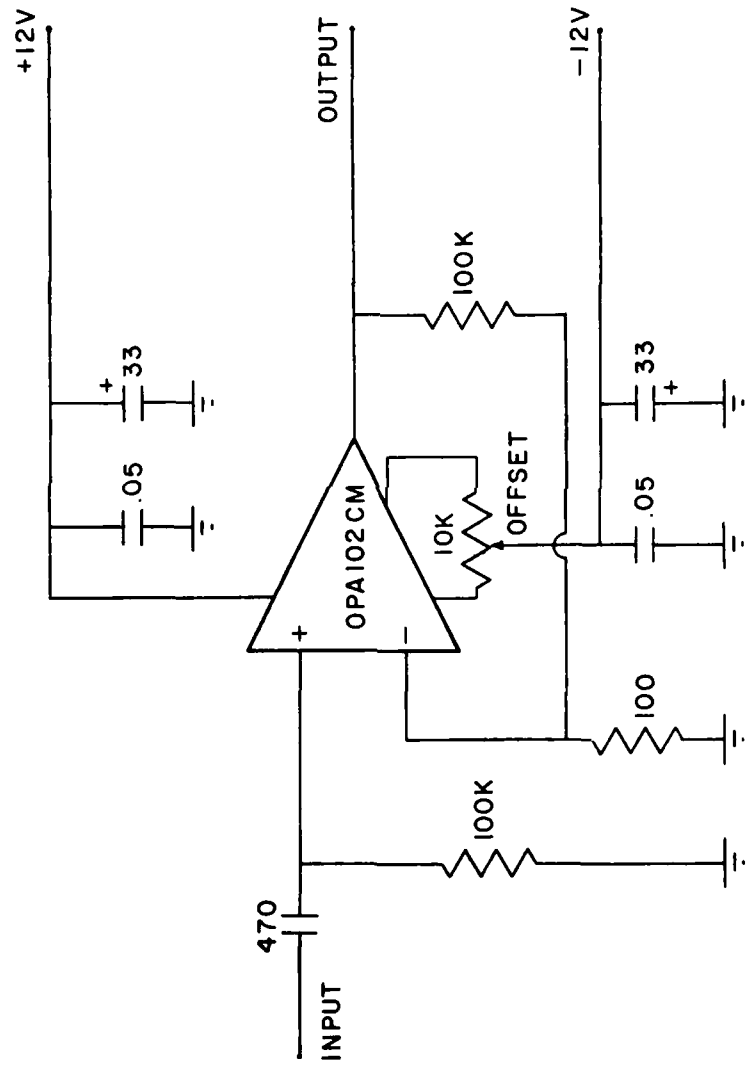


Fig. 6
First main amplifier.

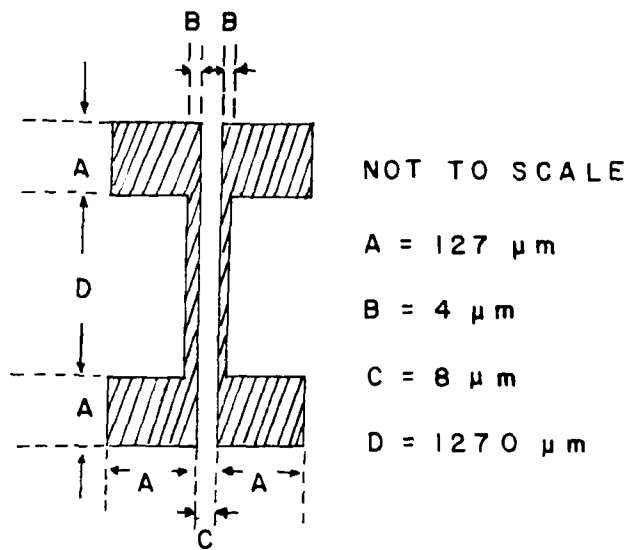


Fig. 7

Layout of films for correlation measurements.

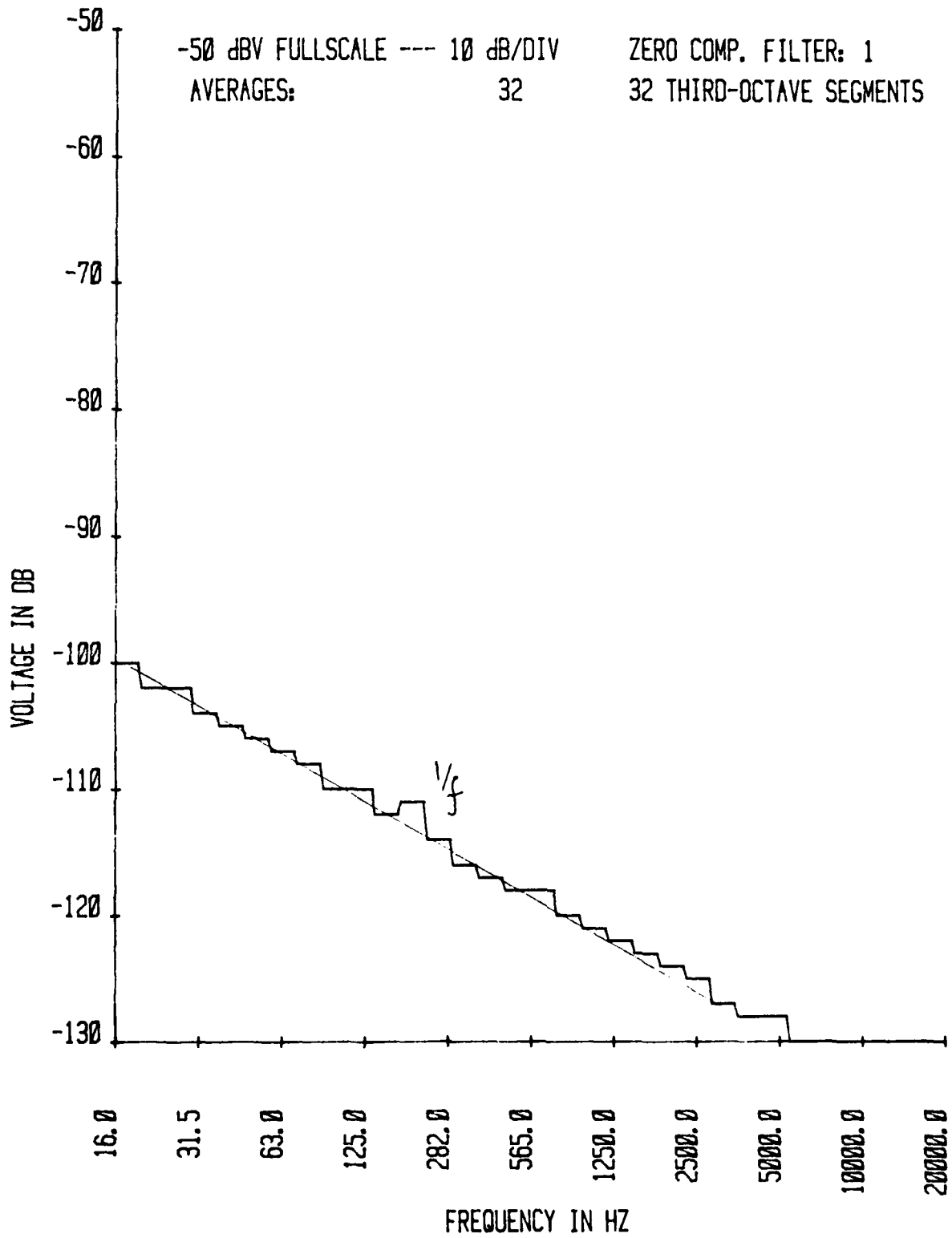


Fig. 8

Noise spectrum of aluminum film at 1.171 mA.

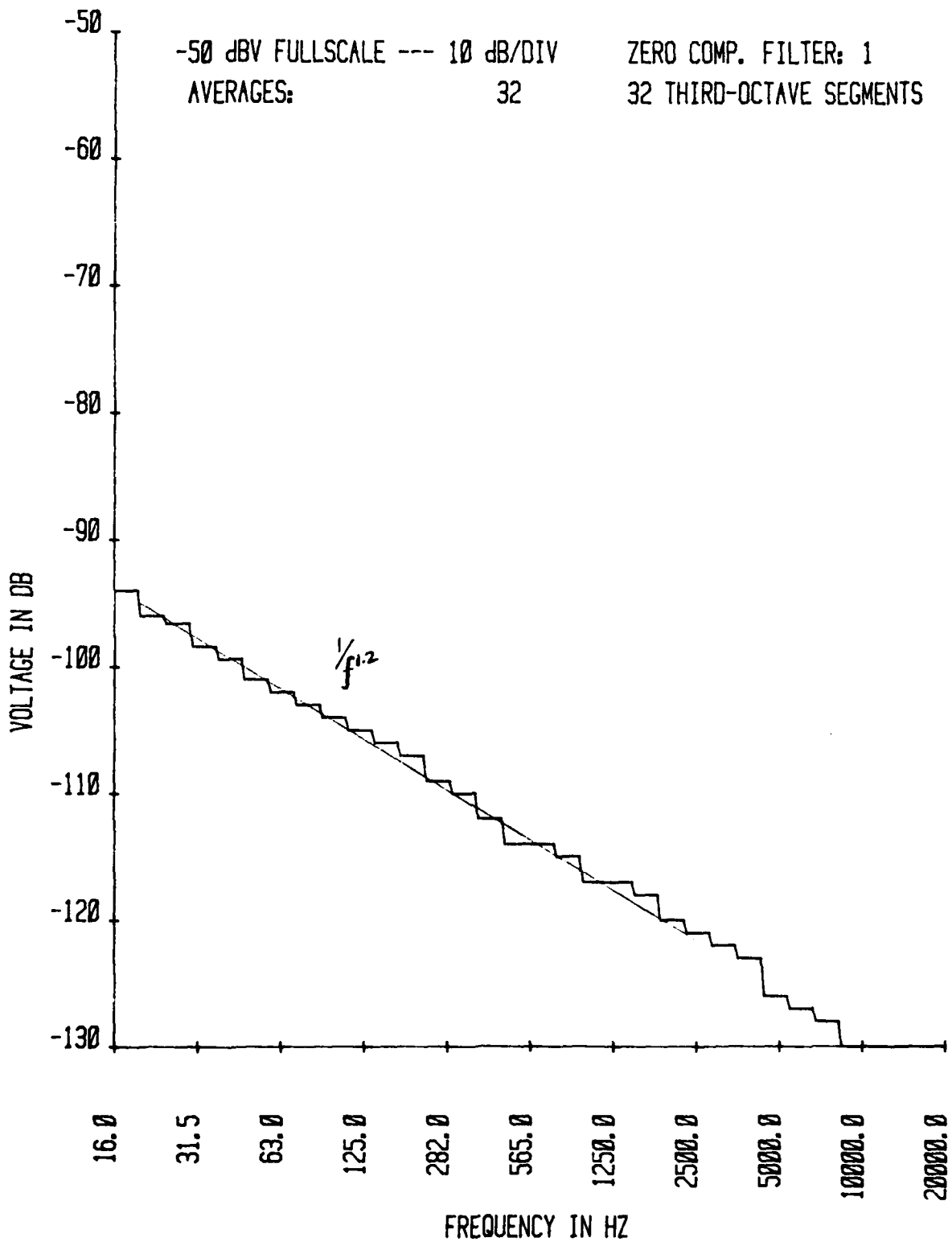


Fig. 9

Noise spectrum of aluminum film at 1.071 mA.

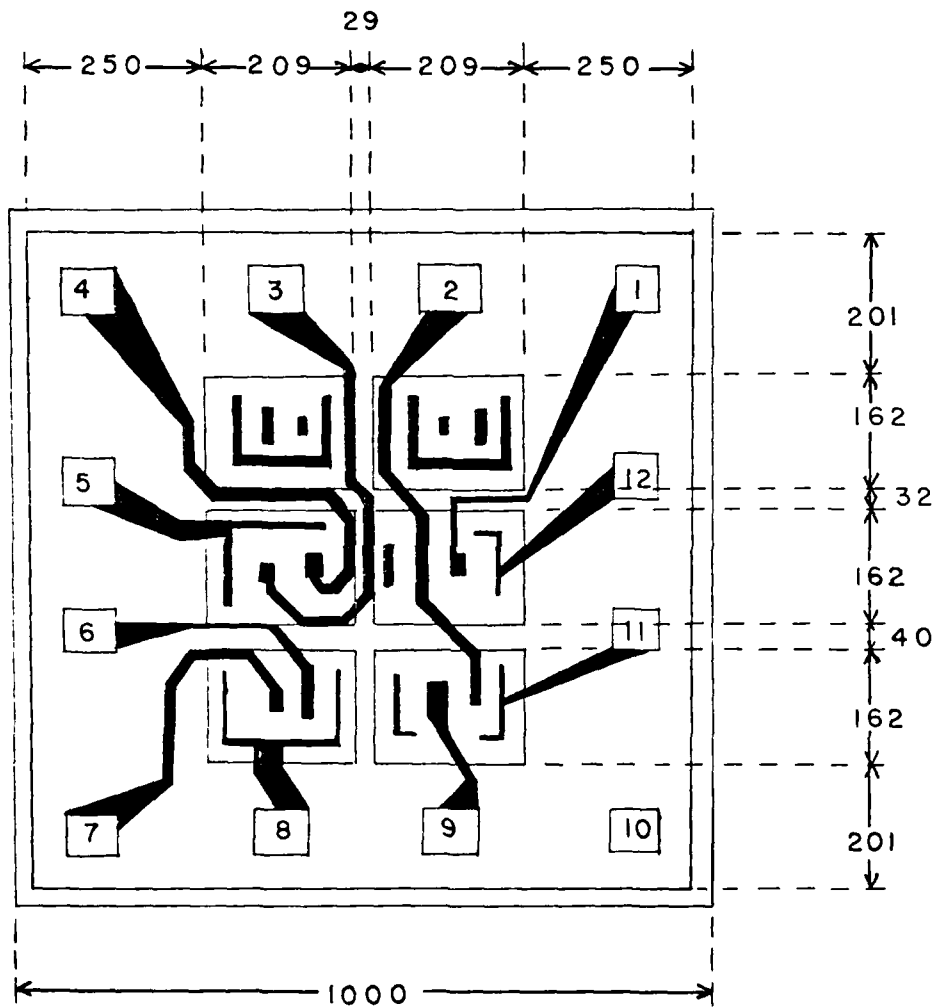


Fig. 11

Top view of integrated circuit CA 3018.

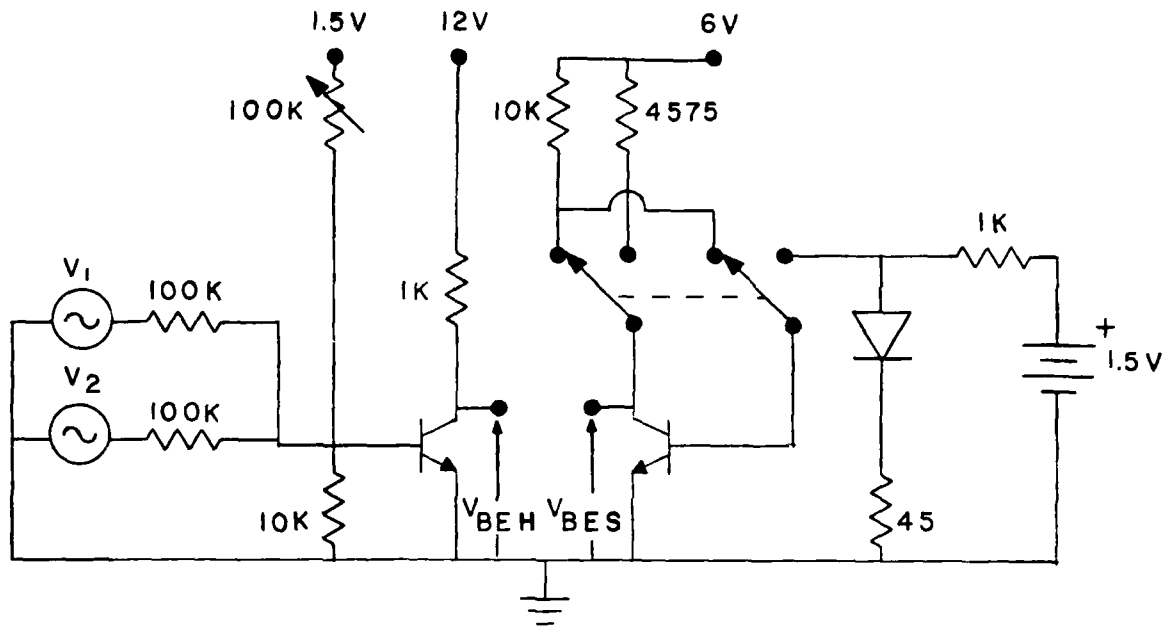


Fig. 12(a)

Circuit for thermal transfer function.

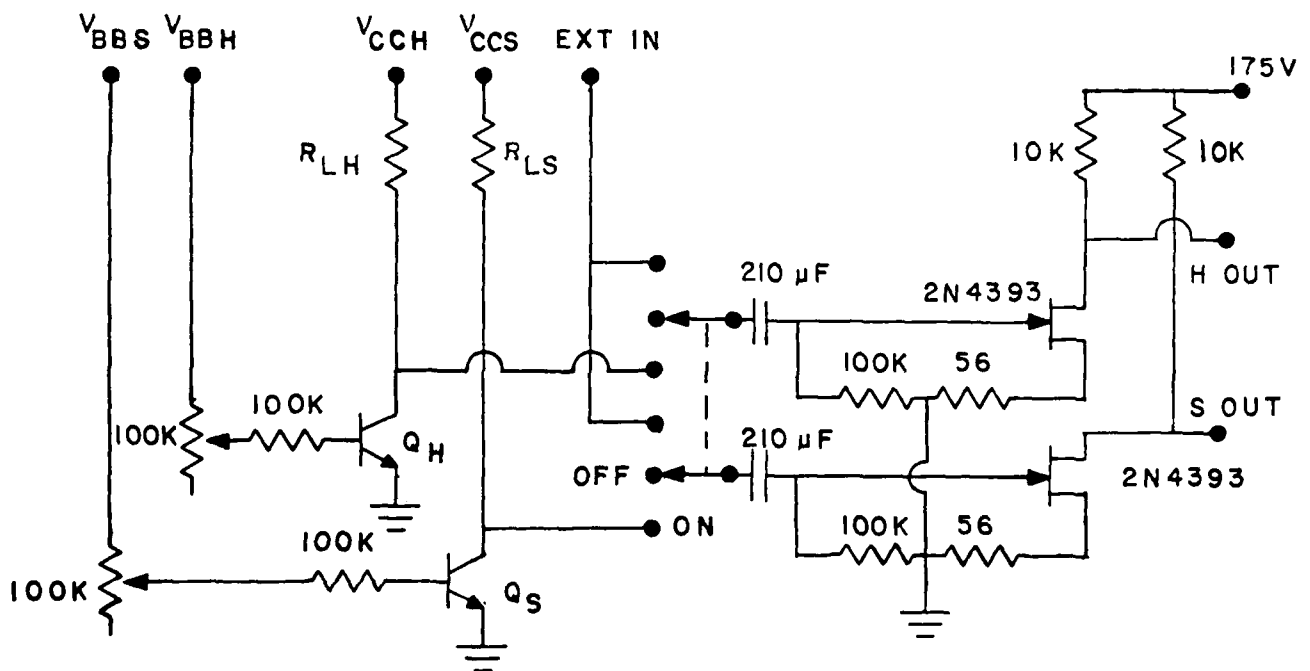


Fig. 12(b)

Circuit to obtain noise spectra and coherence.

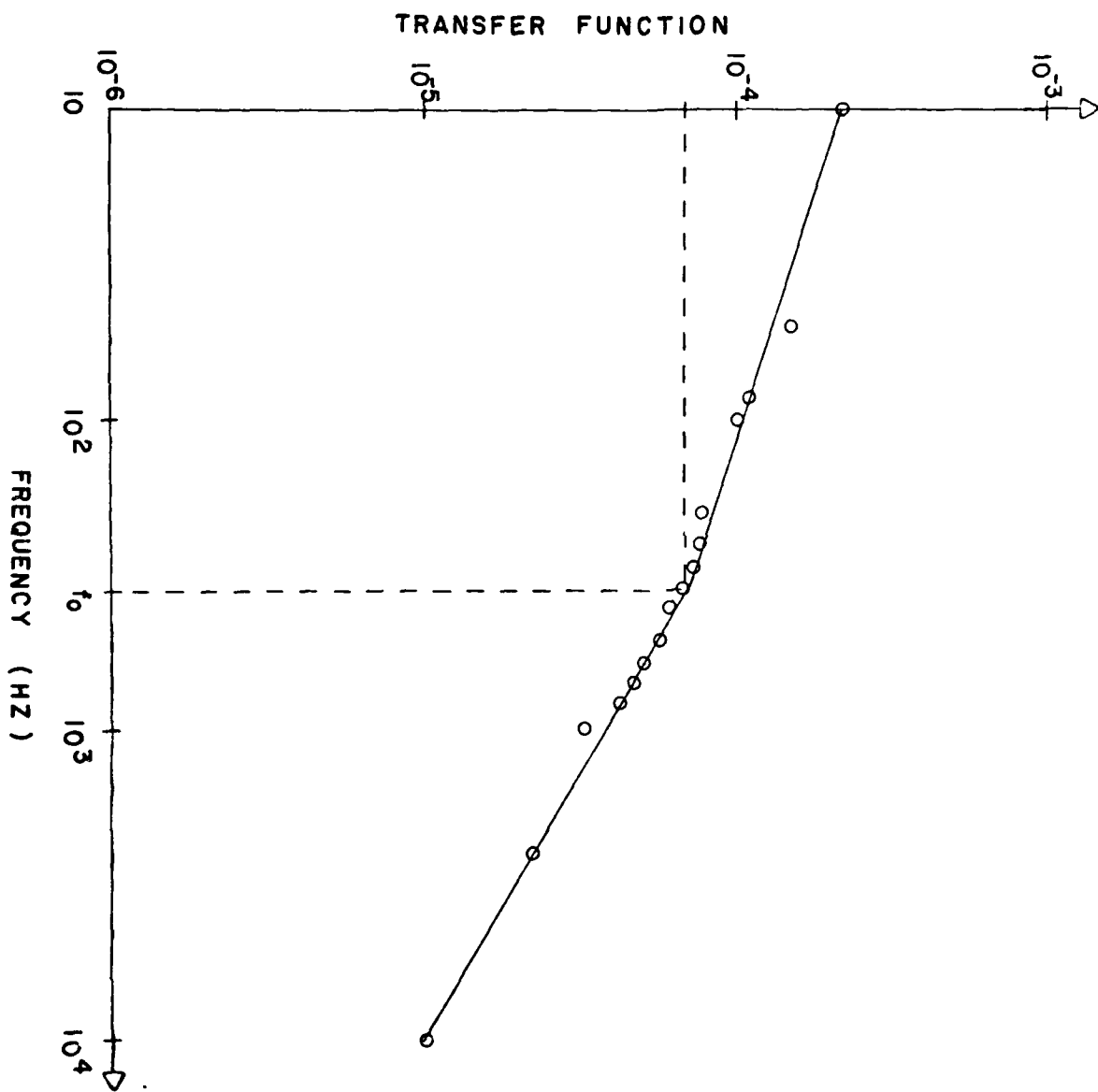


Fig. 13
Thermal transfer function.

COHERENCE: 1.0 FS
AVERAGE: 32
25 KHz /
BW: 726 Hz

.125/DIV
\ 0 Hz

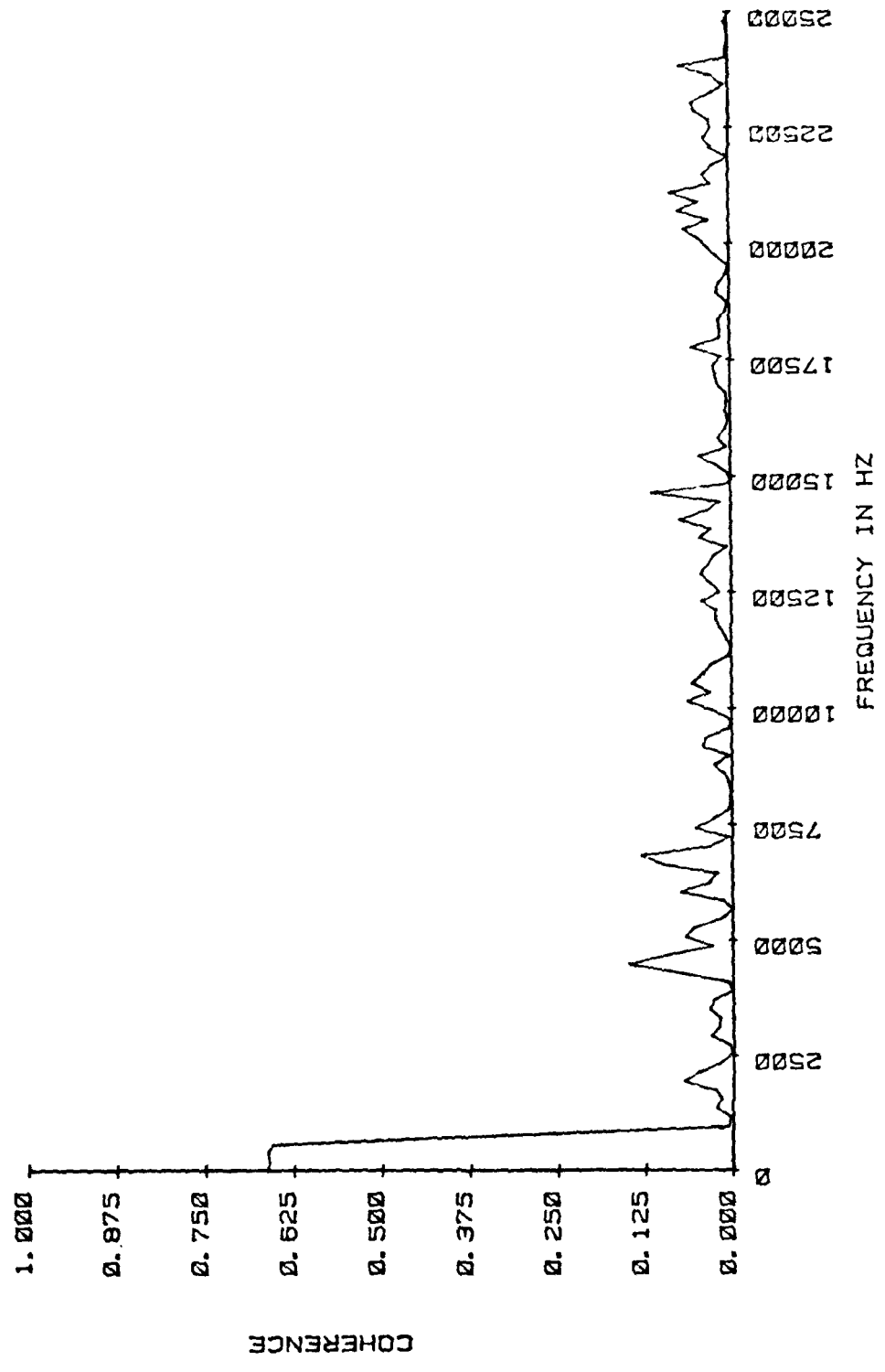


Fig. 14

Correlation of RCA 3018 NPN transistors.

JFET ampl. and wave analyzer

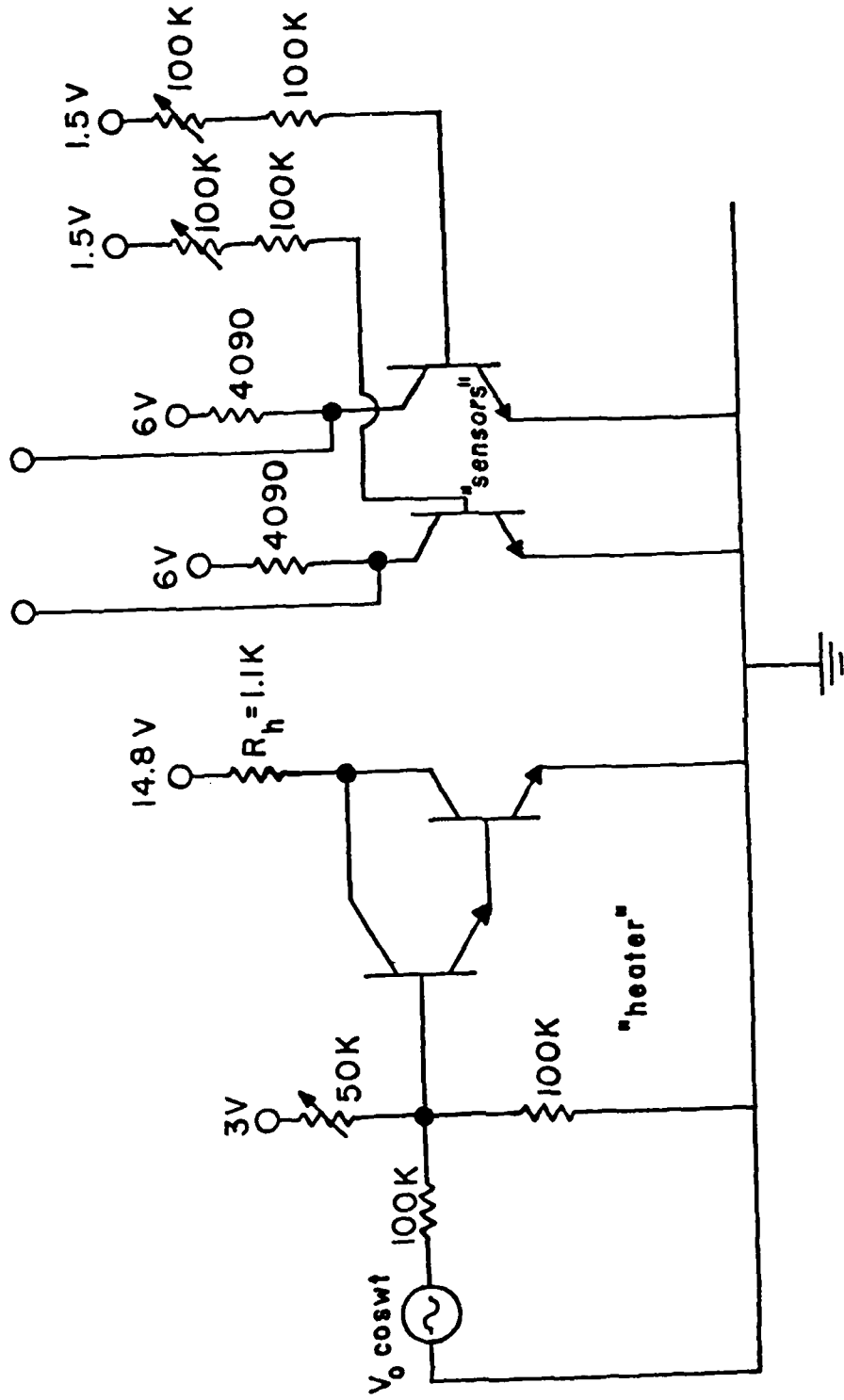


Fig. 15

Three-transistor heat-transfer measurement setup.

TRANSFER FUNCTION

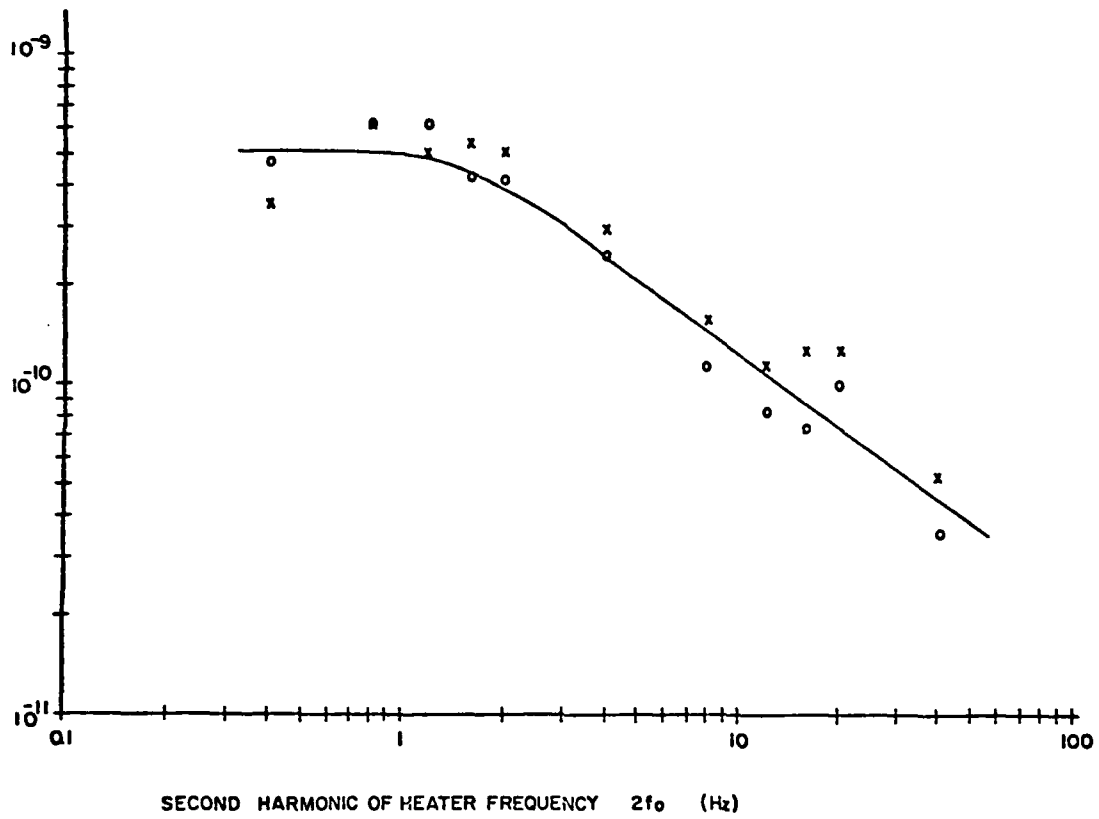


Fig. 16

Thermal transfer function for the two "sensors".

CORRELATION SPECTRUM OF TRANSFER FUNCTION

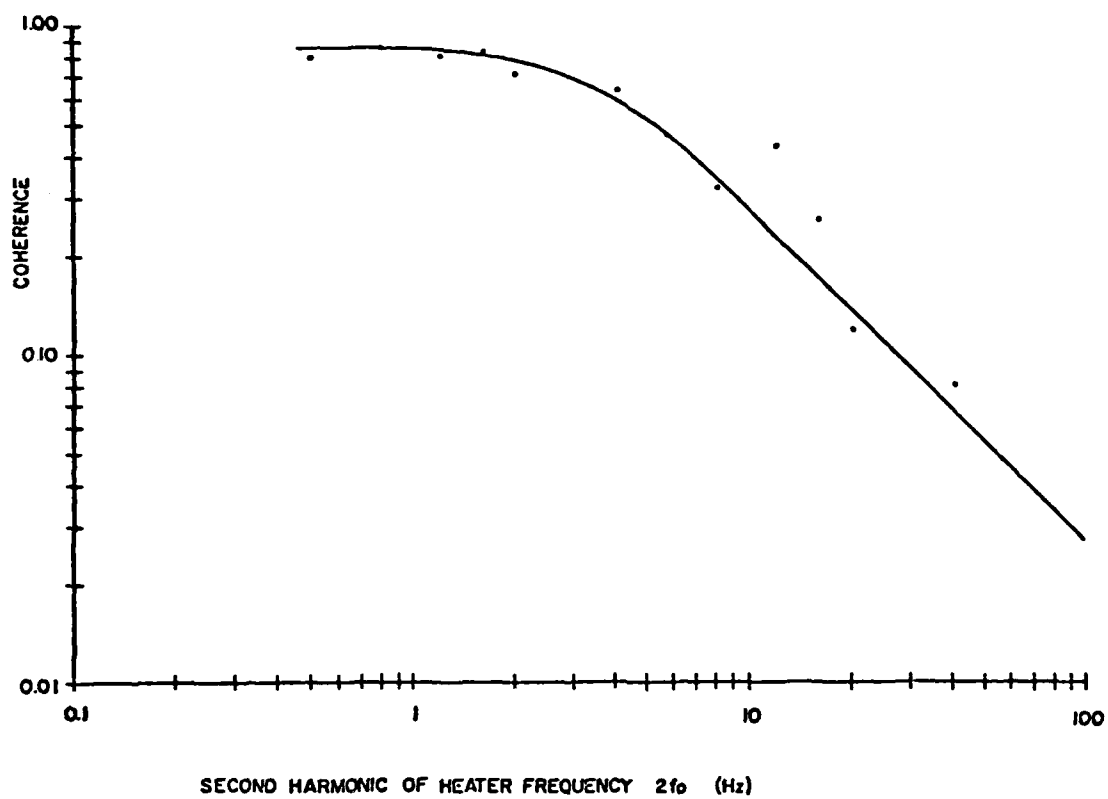


Fig. 17

Correlation (coherence factor) of the two "sensors".

1/f NOISE POWER
(NO HEATER)

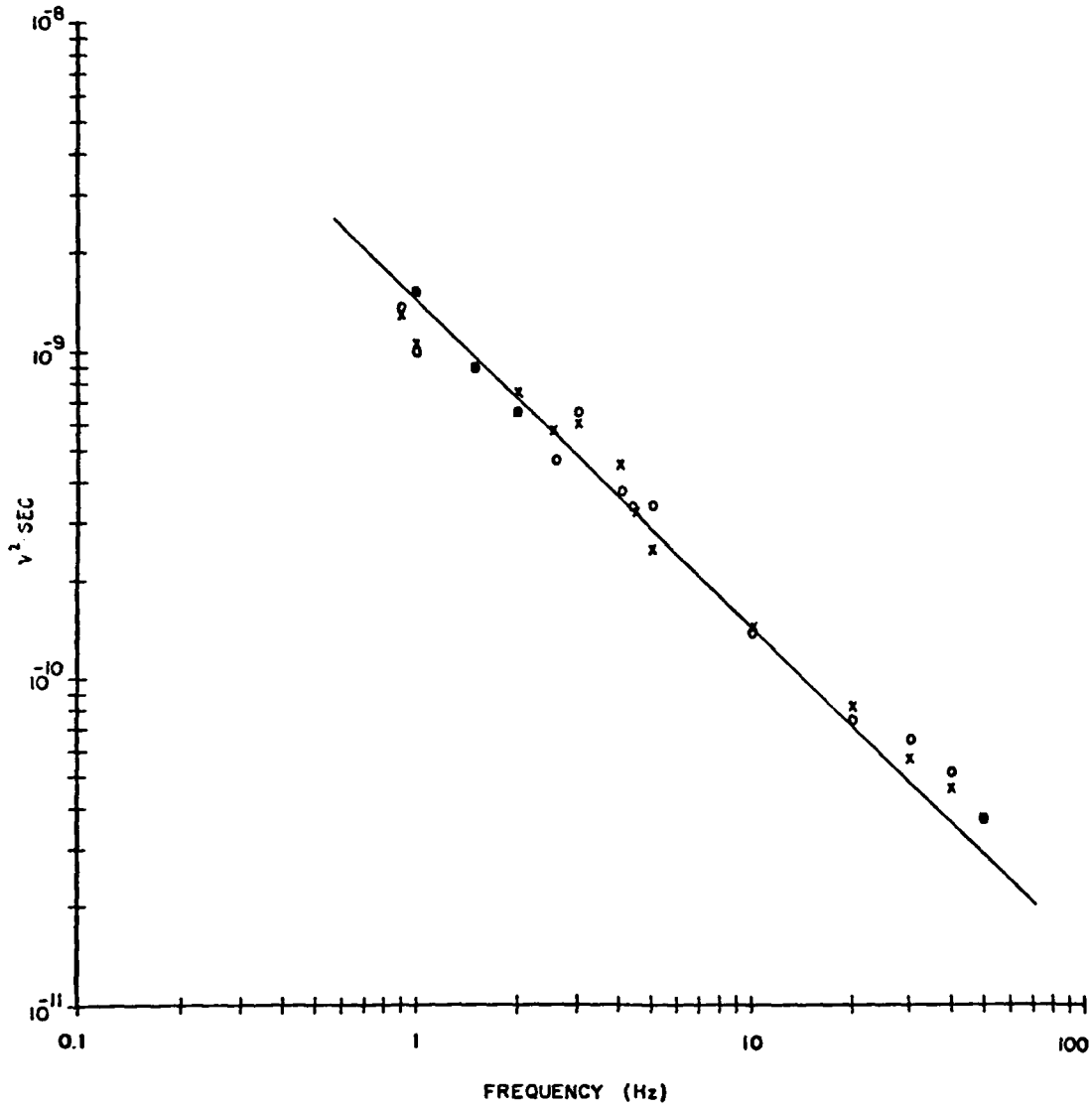


Fig. 18

Noise of the two "sensor" transistors.

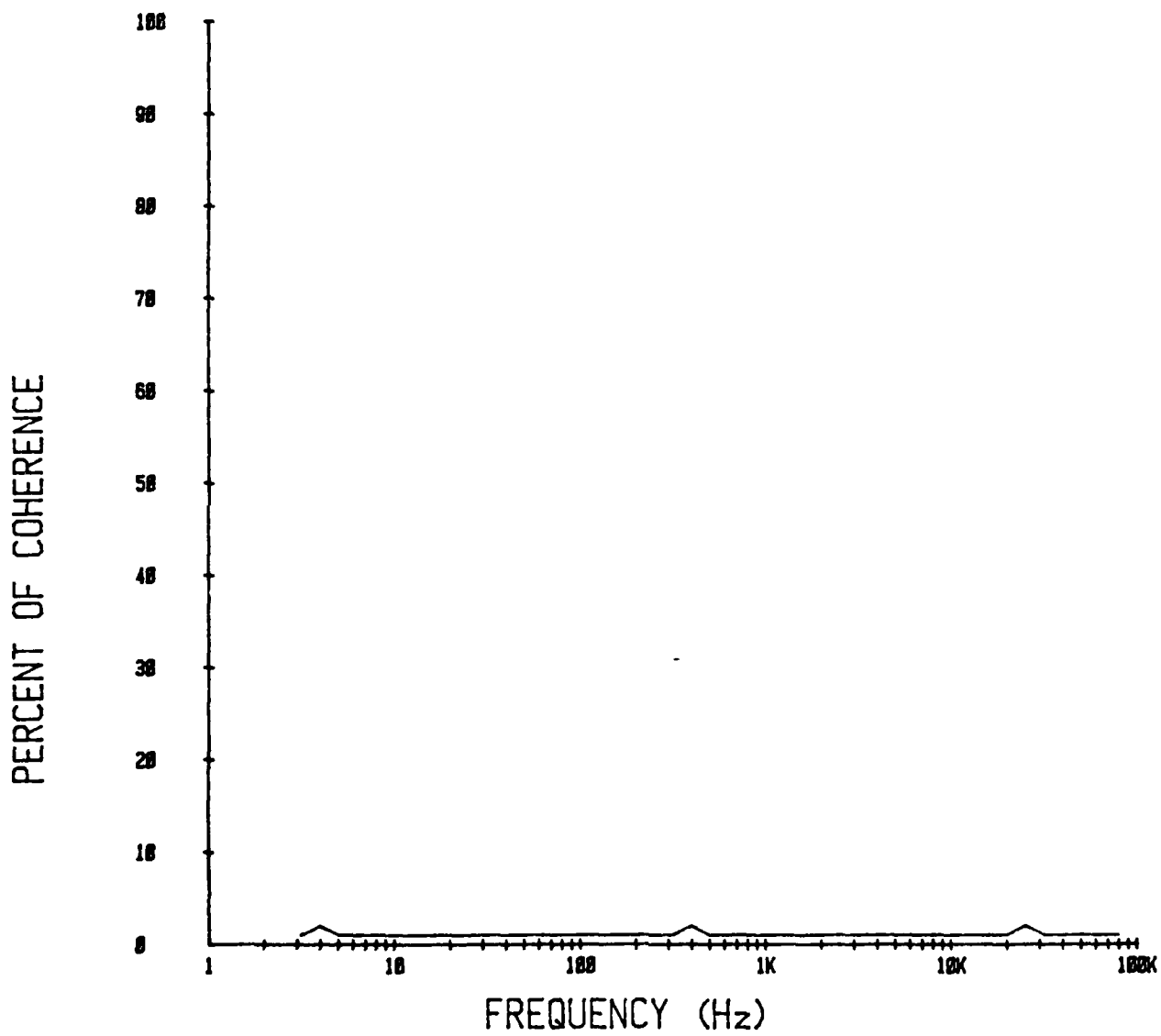


FIG. 19
CORRELATION (COHERENCE FACTOR) OF THE TWO "SENSOR" TRANSISTORS.

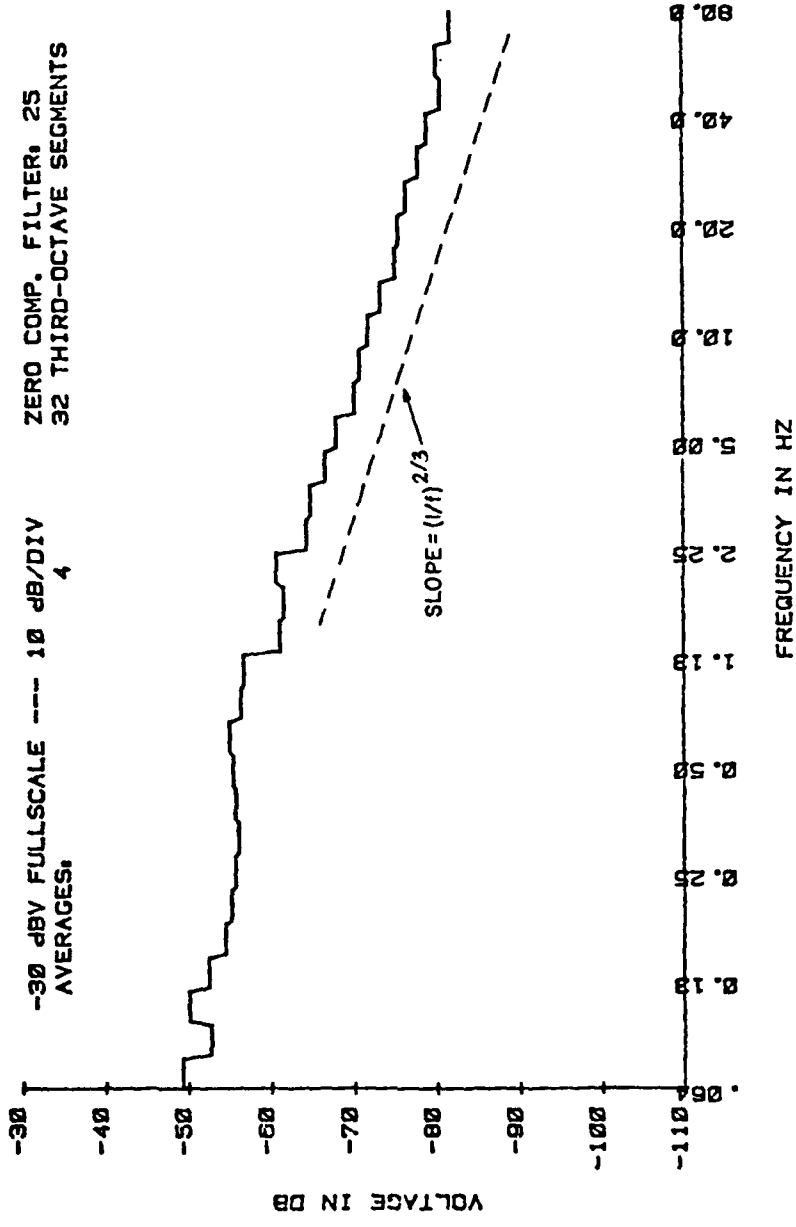


Fig. 21

Low-frequency one-third octave display of collector channel noise
for 2N3945 #1 (see also Fig. 3).

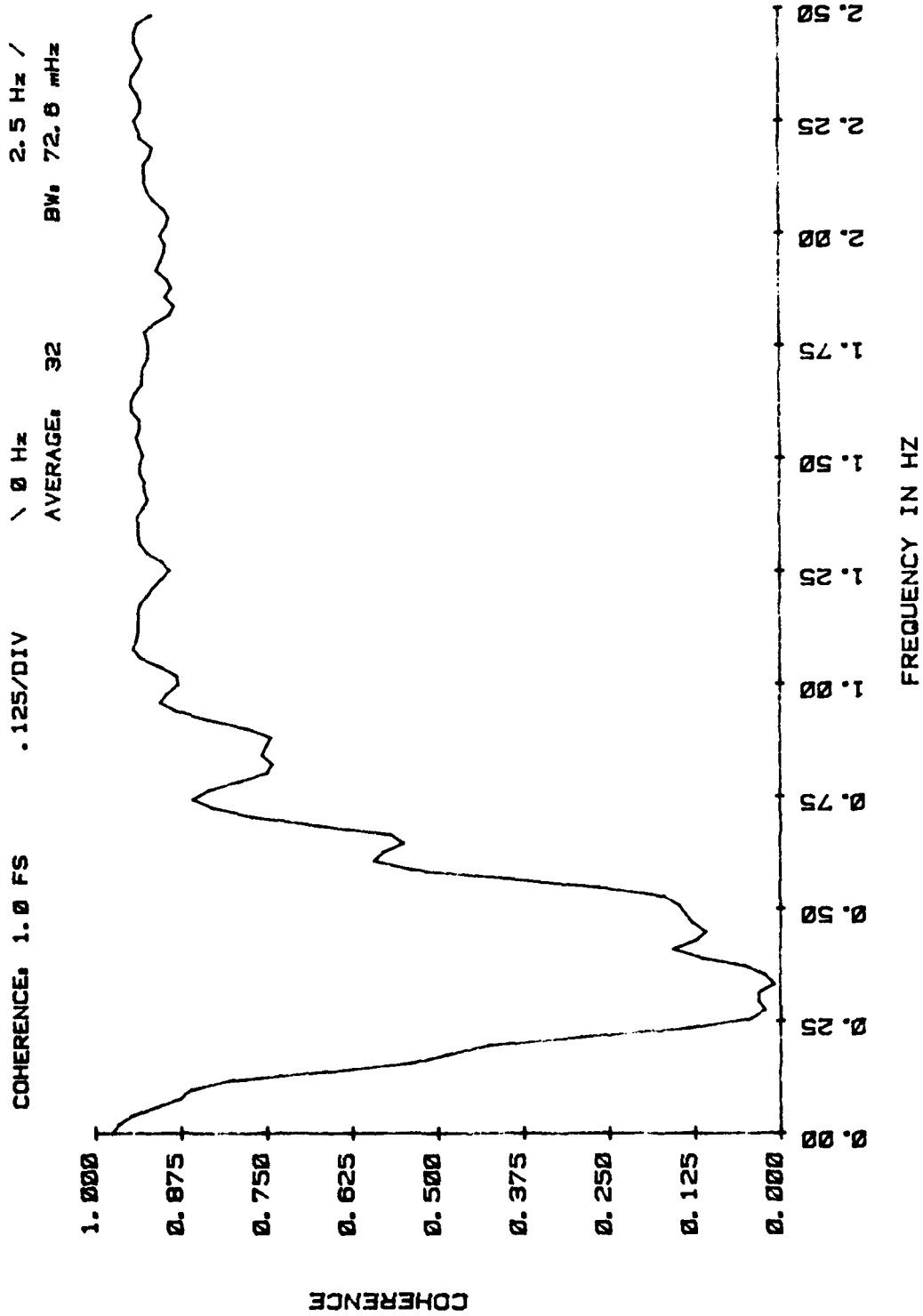


Fig. 22

Low-frequency coherence between collector channel and base channel noise for 2N3945 #1.

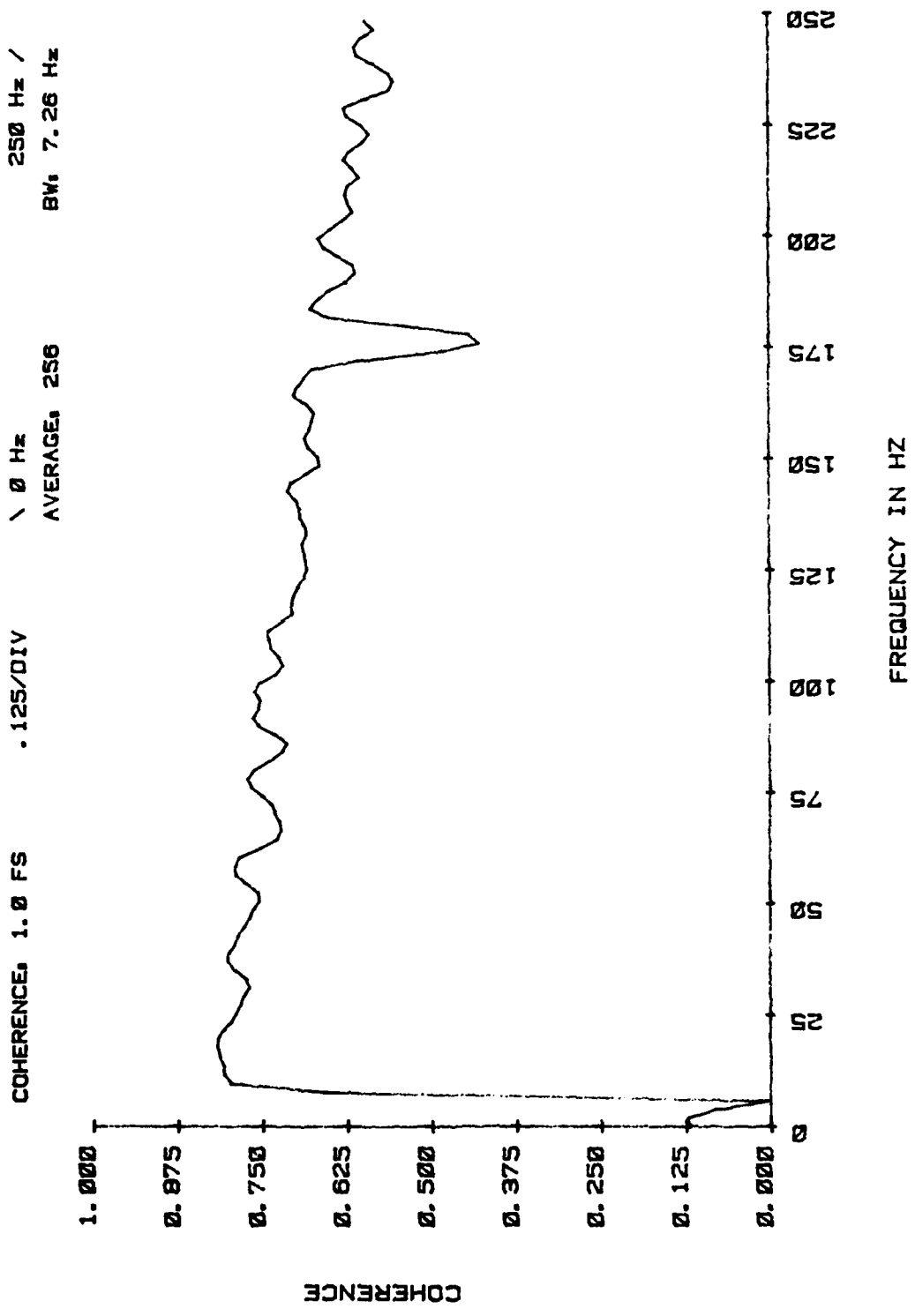


Fig. 23
 One-third octave display of base channel noise for transistor 2N3945 #1.

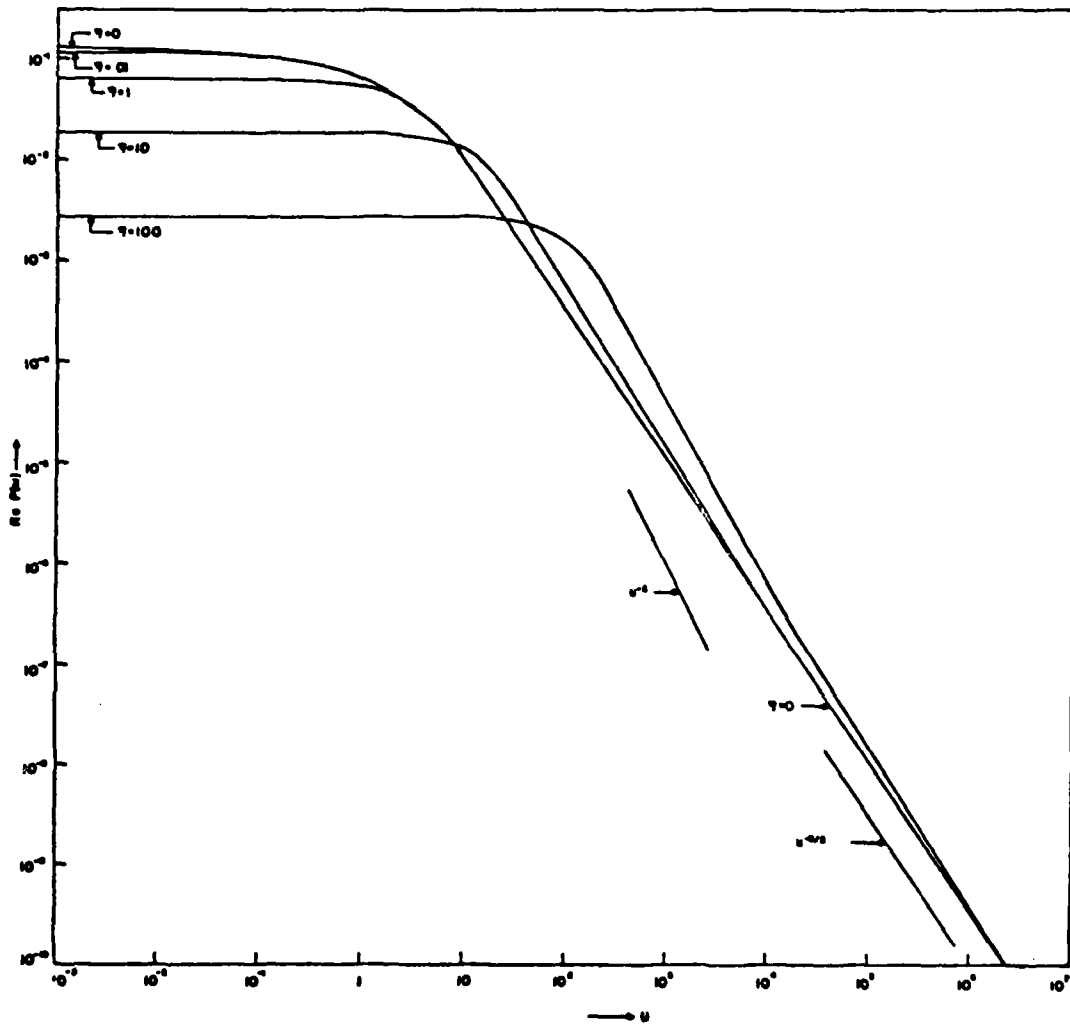


Fig. 24

Noise spectra for embedded sphere ($\eta=0$, $\eta \neq 0$)

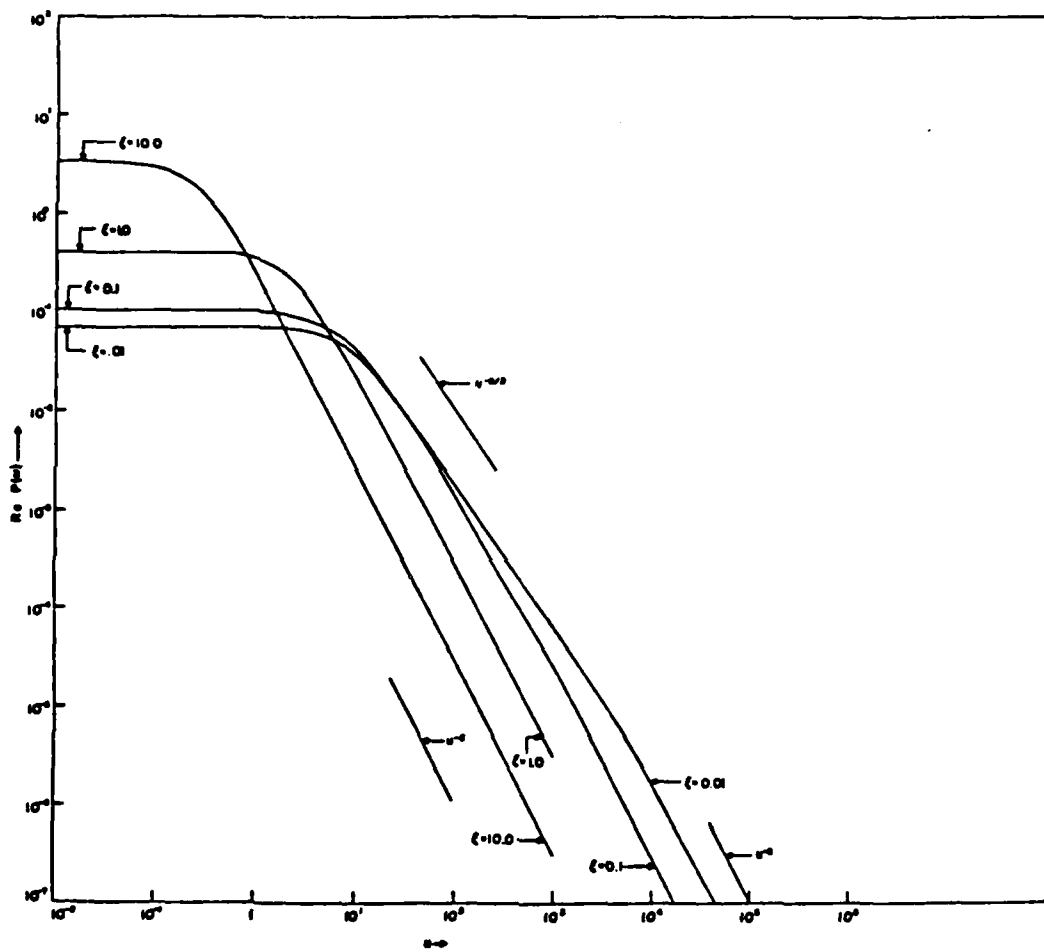


Fig. 25

Noise Spectra for Nonembedded Sphere ($\eta=0$)
 (Slopes indicated are $u^{-3/2}$ and u^{-2})

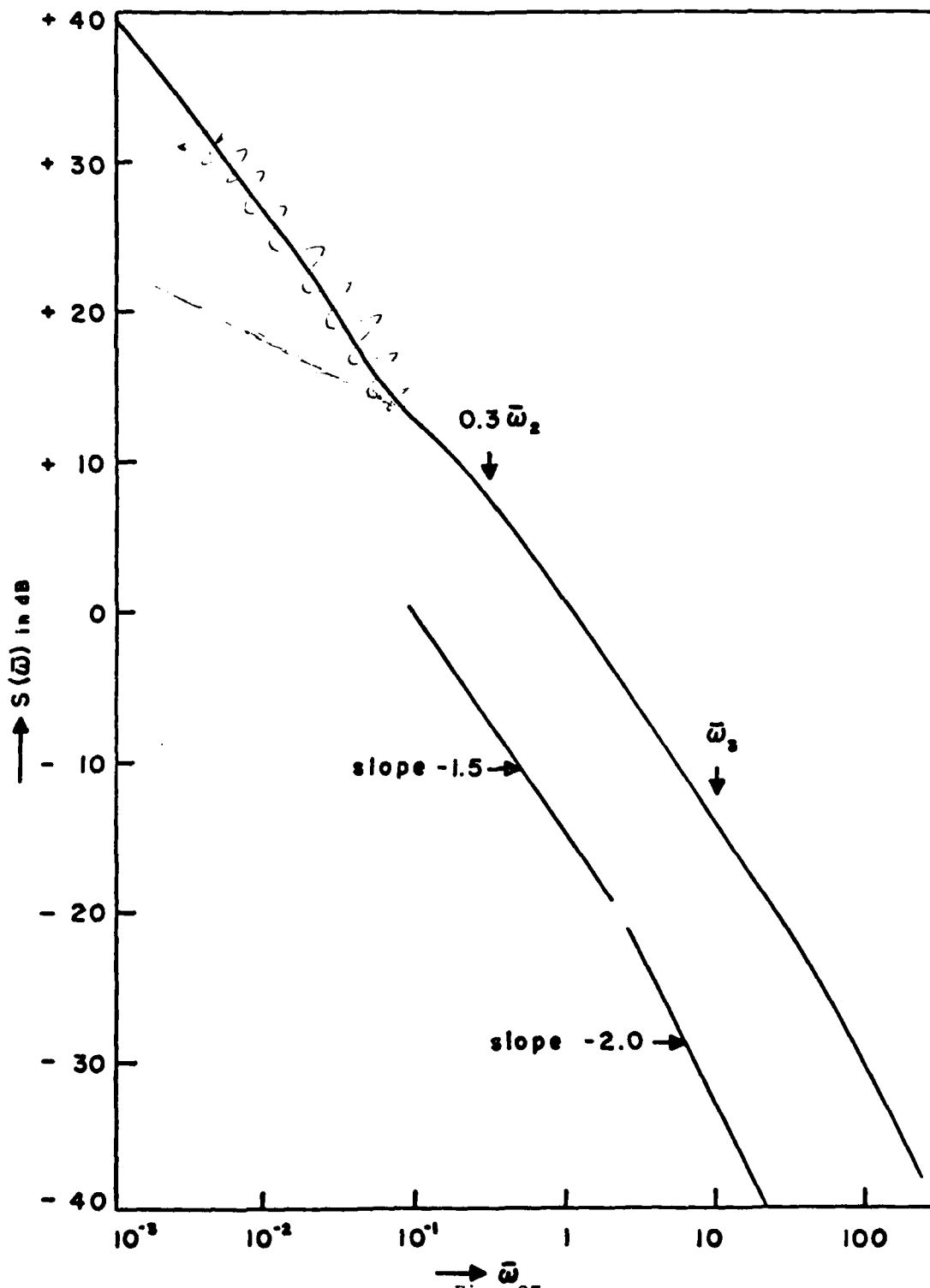


Fig. 27
 Noise spectra for nonsymmetrical bar
 (Voss and Clarke's 'P' noise source)

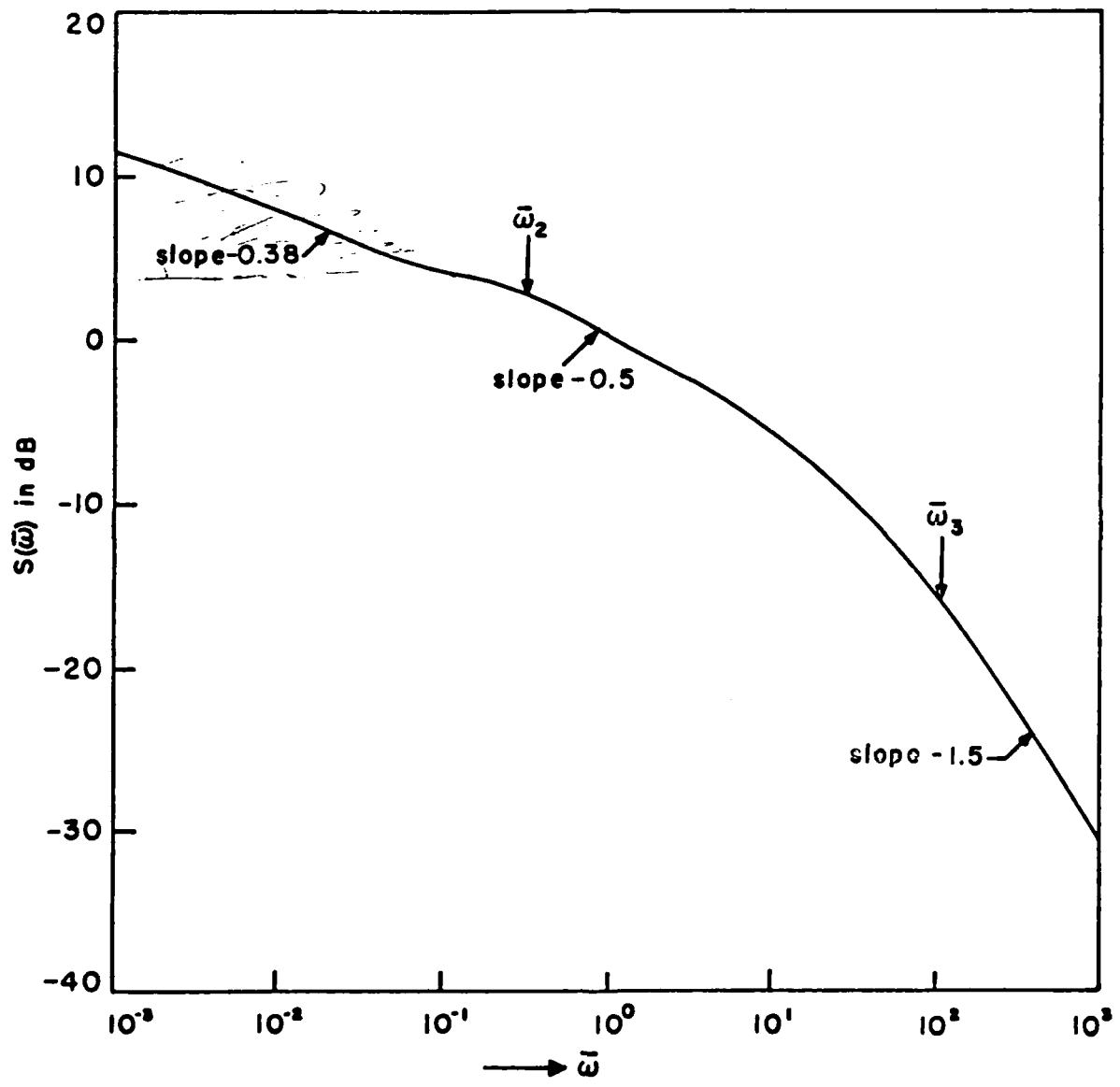


Fig. 28

Noise spectra for nonsymmetrical bar
 (Physical diffusion noise source)

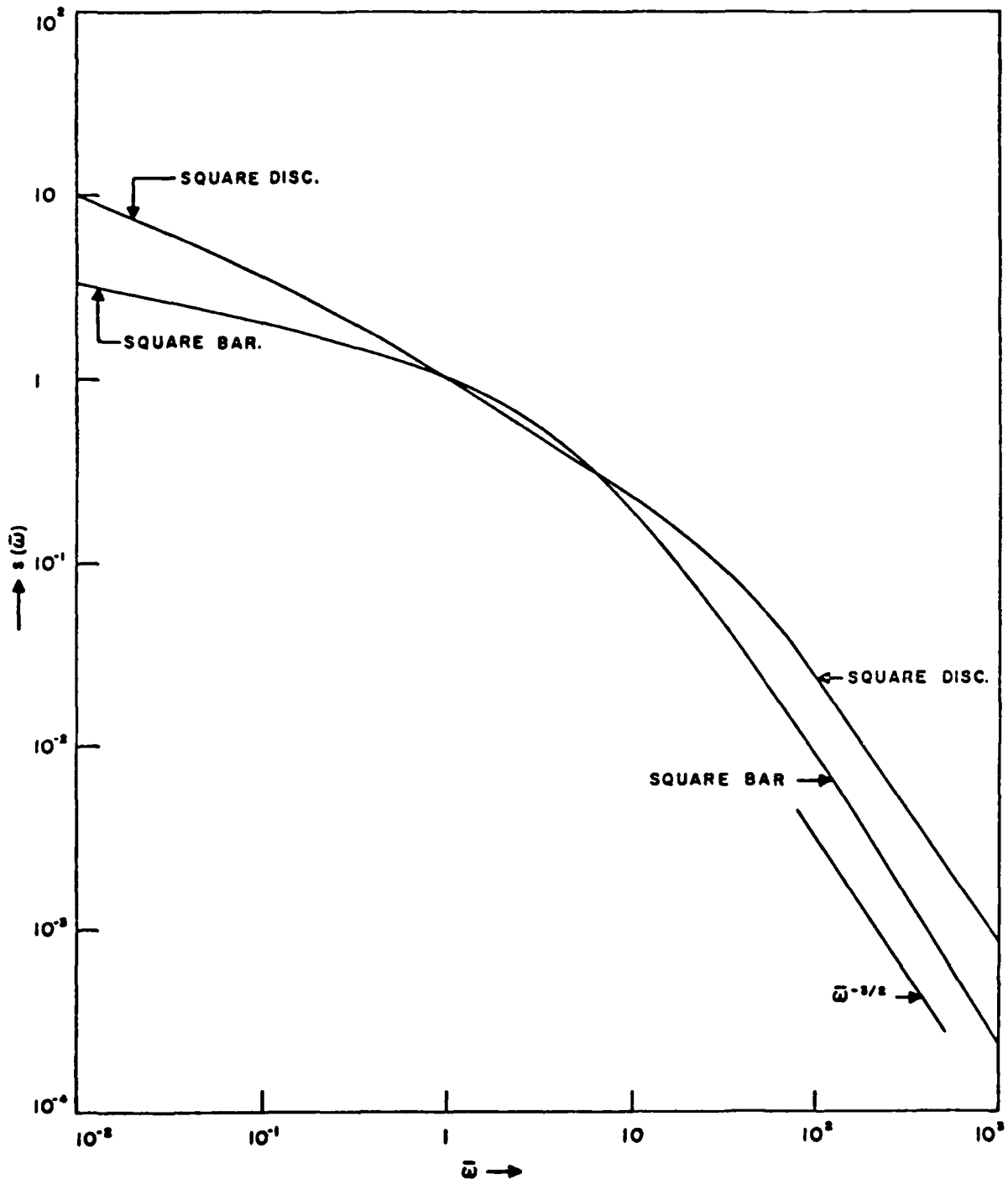


Fig. 29
 Noise spectra for square disc and square bar
 (Physical diffusion noise source)

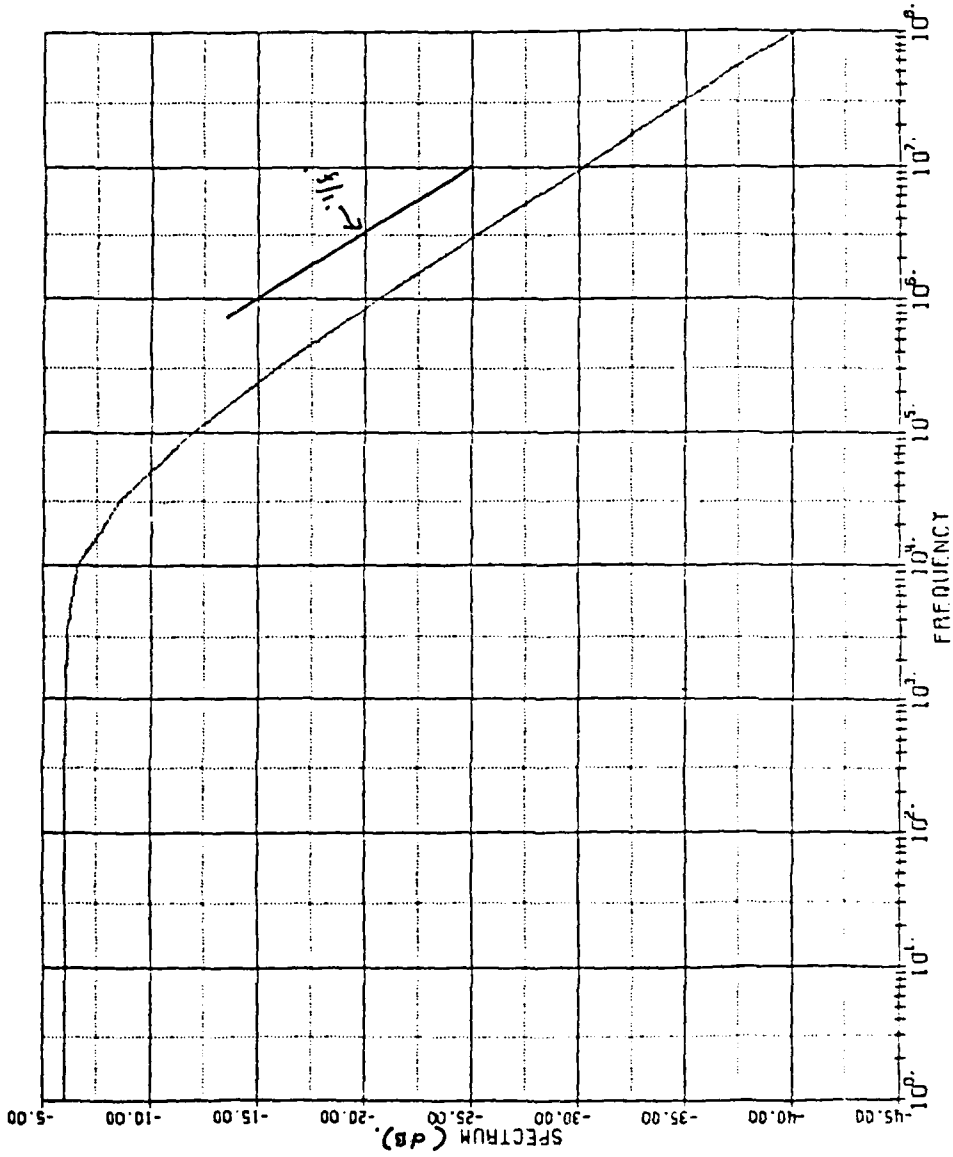


Fig. 30

Noise spectra for a MOSFET due to stochastic surface generation-recombination processes.